

Charge carrier mobility in systems with local electron-phonon interaction

Nikola Prodanović and Nenad Vukmirović*

Scientific Computing Laboratory, Center for the Study of Complex Systems, Institute of Physics Belgrade, University of Belgrade, Pregrevica 118, 11080 Belgrade, Serbia

(Received 9 November 2018; revised manuscript received 12 February 2019; published 18 March 2019)

We present a method for calculation of charge carrier mobility in systems with local electron-phonon interaction. The method is based on unitary transformation of the Hamiltonian to the form where the nondiagonal part can be treated perturbatively. The Green's functions of the transformed Hamiltonian were then evaluated using the Matsubara Green's functions technique. The mobility at low carrier concentration was subsequently evaluated from Kubo's linear response formula. The methodology was applied to investigate the carrier mobility within the one-dimensional Holstein model for a wide range of electron-phonon coupling strengths and temperatures. The results indicated that for low electron-phonon coupling strengths the mobility decreases with increasing temperature, while for large electron-phonon coupling the temperature dependence can exhibit one or two extremal points, depending on the phonon energy. Analytical formulas that describe such behavior were derived. Within a single framework, our approach correctly reproduces the results for mobility in known limiting cases, such as band transport at low temperatures and weak electron-phonon coupling and hopping at high temperatures and strong electron-phonon coupling.

DOI: [10.1103/PhysRevB.99.104304](https://doi.org/10.1103/PhysRevB.99.104304)**I. INTRODUCTION**

Charge carrier mobility is one of the key physical quantities of each material. On the one hand, it determines possible applications of the material in electronic, optoelectronic, and thermoelectric devices. On the other hand, it is an easily measurable quantity that provides information about electronic processes in the material. In the absence of defects and impurities, the mobility of carriers in crystalline materials is fully determined by their interaction with phonons [1]. However, it is rather challenging to calculate phonon-limited mobility for a given material.

The challenge is twofold. On the one hand, it is challenging to construct the Hamiltonian of interacting electrons and phonons. This can be accomplished using density functional perturbation theory [2] which can be used to evaluate relevant electron-phonon coupling constants. However, due to oscillatory dependence of electron-phonon coupling constants on electron and phonon momenta, a dense momentum grid in the Brillouin zone is required [3], which makes these calculations rather time consuming. Significant progress along this line of research has been made since the late 2000s [4–7]. As a consequence of this, in recent years, there have been several reports of *ab initio* mobility calculations in materials where electron-phonon interaction can be treated perturbatively [8–12]. On the other hand, it is also rather challenging to evaluate the mobility for a given Hamiltonian of interacting electrons and phonons. In the cases of weak and strong electron-phonon coupling, perturbative approaches are possible. However, it is significantly more difficult to evaluate the mobility in general case. In this work, we give contribution to this line of research.

We consider a Hamiltonian on the lattice with local electron-phonon interaction, which is a straightforward generalization of a widely studied Holstein model [13]. In the case of weak electron-phonon interaction the problem can be analyzed using a perturbative approach. It is known that Lang-Firsov unitary transformation [14] exactly diagonalizes the Hamiltonian in the limit of infinitely large electron-phonon interaction and therefore it can be used as a starting point for perturbative approach for strong electron-phonon interaction. It is, however, unclear how to tackle the problem for intermediate values of electron-phonon interaction. A variety of theoretical methods, such as exact diagonalization [15–17], density matrix renormalization group [18–20], variational approaches [21–25], dynamical mean-field theory [26,27], and quantum Monte Carlo [25,28–31], was used to study the Holstein and related models. However, most of these methods were focused on evaluation of the ground state of the system and very little effort was focused on more challenging evaluation of correlation functions at finite temperature. It is only recently that quantum Monte Carlo calculation of finite-temperature mobility within the Holstein model was performed [32]. Zero-temperature optical conductivity was analyzed in Refs. [33] and [34], while temperature dependence of resistivity within dynamical mean-field theory was investigated in Ref. [27].

In this work, we present the method for evaluation of mobility in systems with local electron-phonon interaction. The first step in our procedure is based on unitary transformation of the Hamiltonian. The parameters of the transformation were chosen in such a way that the nondiagonal part of the Hamiltonian is minimized in a certain sense. Next, relevant self-energies and spectral functions of the transformed Hamiltonian were evaluated using Matsubara Green's function formalism by keeping the lowest-order nonzero term in

*nenad.vukmirovic@ipb.ac.rs

the expansion. The spectral functions were subsequently used as input to evaluate the mobility using Kubo's linear response formula. We illustrate the methodology by performing the calculation of mobility for Holstein model in one dimension for a wide range of model parameters.

The idea of calculating the mobility or diffusivity by combining unitary transformation of the Hamiltonian with evaluation of correlation function for the transformed Hamiltonian has been followed in different studies in the past [35–40]. The main advantage of our approach over these approaches is that we capture the time decay of current-current correlation function without introducing additional phenomenological parameters extrinsic to the model Hamiltonian. As a consequence of this, we do not obtain singularities that would lead to infinite mobility. More details of the comparison of our approach with other related works is given in Sec. IV.

The paper is organized as follows. In Sec. II we present the overall theoretical framework of our method. In particular, in Sec. II A we introduce the Hamiltonian that we consider and its unitary transformation. The procedure for evaluating self-energies and spectral functions is presented in Sec. II B, while the expressions for mobility calculation are derived in Sec. II C. In Sec. III we illustrate the method by applying it to one-dimensional Holstein model for a wide range of model parameters. We first briefly discuss numerical aspects in Sec. III A. We present the results for parameters of unitary transformation and the spectral function of transformed Hamiltonian in Sec. III B. The results obtained for mobility are given in Sec. III C, along with analytical formulas in several limiting cases. In Sec. IV we additionally compare our approach with other related papers and discuss the range of applicability of our approach and its possible extensions.

II. THEORETICAL CONSIDERATIONS

A. The Hamiltonian and its unitary transformation

We consider the Hamiltonian

$$H = H_e + H_{\text{ph}} + H_{e-\text{ph}}, \quad (1)$$

where

$$H_e = - \sum_{\mathbf{R}, \mathbf{S}} J_{\mathbf{R}-\mathbf{S}} a_{\mathbf{R}}^\dagger a_{\mathbf{S}} \quad (2)$$

is the electronic part of the Hamiltonian,

$$H_{\text{ph}} = \sum_{\mathbf{R}, f} \hbar \Omega_f b_{\mathbf{R}, f}^\dagger b_{\mathbf{R}, f} \quad (3)$$

is the part that describes phonons, while

$$H_{e-\text{ph}} = \sum_{\mathbf{R}, f} G_f a_{\mathbf{R}}^\dagger a_{\mathbf{R}} (b_{\mathbf{R}, f}^\dagger + b_{\mathbf{R}, f}) \quad (4)$$

is the electron-phonon interaction Hamiltonian. In previous equations, the indices \mathbf{R} and \mathbf{S} denote the positions of lattice sites, $a_{\mathbf{R}}^\dagger$ and $a_{\mathbf{R}}$ are electron creation and annihilation operators at site \mathbf{R} , while $J_{\mathbf{R}-\mathbf{S}}$ is electronic transfer integral between sites \mathbf{R} and \mathbf{S} . It is assumed that at lattice site \mathbf{R} there is a finite number of localized phonon modes of energy $\hbar \Omega_f$ that are labeled by index f . The corresponding creation and annihilation operators for phonons in these modes are $b_{\mathbf{R}, f}^\dagger$

and $b_{\mathbf{R}, f}$. The parameter G_f quantifies the interaction between an electron at site \mathbf{R} and the phonon mode f at the same site.

To transform the Hamiltonian to a more convenient form where interacting term can be treated perturbatively, we perform a unitary transformation of the Hamiltonian

$$\tilde{H} = U^{-1} H U, \quad (5)$$

where unitary operator U is given as [38]

$$U = e^{\sum_{\mathbf{R}} a_{\mathbf{R}}^\dagger a_{\mathbf{R}} \sum_{\mathbf{S}, f} D_{\mathbf{S}, f} (b_{\mathbf{R}+\mathbf{S}, f} - b_{\mathbf{R}, f}^\dagger)}. \quad (6)$$

This transformation is a generalization of the Lang-Firsov unitary transformation [14] and follows a similar idea used in early studies of continuum Fröhlich polaron [41]. Parameters of the transformation $D_{\mathbf{S}, f}$ will be chosen to minimize the interaction term in certain sense, as will be described in the next paragraph. After transformation the Hamiltonian takes the form

$$\tilde{H} = \tilde{H}_0 + \tilde{V}, \quad (7)$$

where the noninteracting term \tilde{H}_0 reads

$$\tilde{H}_0 = \sum_{\mathbf{k}} E_{\mathbf{k}} a_{\mathbf{k}}^\dagger a_{\mathbf{k}} + \sum_{\mathbf{R}, f} \hbar \Omega_f b_{\mathbf{R}, f}^\dagger b_{\mathbf{R}, f} \quad (8)$$

with

$$a_{\mathbf{k}} = \frac{1}{\sqrt{N_k}} \sum_{\mathbf{R}} a_{\mathbf{R}} e^{i\mathbf{k}\cdot\mathbf{R}}, \quad (9)$$

$$E_{\mathbf{k}} = - \sum_{\mathbf{R}} J_{\mathbf{R}} e^{i\mathbf{k}\cdot\mathbf{R}} \theta_{\mathbf{R}}^{(0)} + E', \quad (10)$$

$$E' = \sum_{\mathbf{R}, f} \hbar \Omega_f D_{\mathbf{R}, f}^2 - 2 \sum_f G_f D_{0, f}, \quad (11)$$

$$\theta_{\mathbf{R}}^{(0)} = e^{-\sum_{\mathbf{S}, f} (D_{\mathbf{S}, f} - D_{\mathbf{S}-\mathbf{R}, f})^2 (n_f^{\text{ph}} + \frac{1}{2})}, \quad (12)$$

and

$$n_f^{\text{ph}} = \frac{1}{e^{\frac{\hbar \Omega_f}{k_B T}} - 1} \quad (13)$$

is the phonon occupation number at temperature T , while N_k is the number of lattice sites. The interaction term reads

$$\tilde{V} = \frac{1}{N_k} \sum_{\mathbf{k}, \mathbf{q}} a_{\mathbf{k}+\mathbf{q}}^\dagger a_{\mathbf{k}} \mathcal{B}_{\mathbf{k}, \mathbf{q}}, \quad (14)$$

where $\mathcal{B}_{\mathbf{k}, \mathbf{q}} = \mathcal{B}_{\mathbf{k}, \mathbf{q}}^{(1)} + \mathcal{B}_{\mathbf{k}, \mathbf{q}}^{(2)}$ and

$$\mathcal{B}_{\mathbf{k}, \mathbf{q}}^{(1)} = \sum_{\mathbf{R}, f} e^{i\mathbf{q}\cdot\mathbf{R}} \left(G_f - \hbar \Omega_f \sum_{\mathbf{S}} D_{\mathbf{S}, f} e^{-i\mathbf{q}\cdot\mathbf{S}} \right) (b_{\mathbf{R}, f} + b_{\mathbf{R}, f}^\dagger), \quad (15)$$

$$\mathcal{B}_{\mathbf{k}, \mathbf{q}}^{(2)} = - \sum_{\mathbf{R}, \mathbf{S}} J_{\mathbf{R}-\mathbf{S}} e^{i(\mathbf{k}+\mathbf{q})\cdot\mathbf{R}-\mathbf{k}\cdot\mathbf{S}} [\theta_{\mathbf{R}}^\dagger \theta_{\mathbf{S}} - \theta_{\mathbf{R}-\mathbf{S}}^{(0)}], \quad (16)$$

with

$$\theta_{\mathbf{R}} = e^{\sum_{\mathbf{S}, f} D_{\mathbf{S}, f} (b_{\mathbf{S}+\mathbf{R}, f} - b_{\mathbf{S}, f}^\dagger)}. \quad (17)$$

Next we discuss the procedure for choosing the parameters of the unitary transformation $D_{\mathbf{R}, f}$. First, we note that free energy of the system is invariant under unitary transformation.

Therefore it can be expressed as $F = -k_B T \ln \text{Tr} e^{-\beta \tilde{H}}$, where $\beta = \frac{1}{k_B T}$. Next we utilize Gibbs-Bogoliubov inequality [42]

$$-k_B T \ln \text{Tr} e^{-\beta \tilde{H}} \leq \text{Tr}(\rho_t \tilde{H}) + k_B T \text{Tr}(\rho_t \ln \rho_t) \quad (18)$$

that is valid for any statistical operator ρ_t . By choosing ρ_t in the form

$$\rho_t = \frac{e^{-\beta \tilde{H}_0}}{\text{Tr} e^{-\beta \tilde{H}_0}} \quad (19)$$

we arrive at

$$F \leq -k_B T \ln \text{Tr} e^{-\beta \tilde{H}_0}. \quad (20)$$

Equation (20) gives an upper bound on the free energy of the system $F_{ub} = -k_B T \ln \text{Tr} e^{-\beta \tilde{H}_0}$ which is equal to the free energy of the noninteracting system described by the Hamiltonian \tilde{H}_0 , which depends on the parameters of the unitary transformation $D_{\mathbf{R},f}$. We choose these parameters to minimize F_{ub} . With such a choice of parameters the upper bound on the free energy F_{ub} will be closest to free energy of the system F and the effect of interaction \tilde{V} in Eq. (7) will be minimized. It is then expected that perturbative treatment of interaction \tilde{V} is possible. Evaluation of F_{ub} is possible, since it is equal to the free energy of the noninteracting system. Explicit expression for F_{ub} and the equations for optimal parameters of the unitary transformation in the case of a one-dimensional model with nearest-neighbor interaction are given in Appendix A.

B. Self-energies and spectral functions

To evaluate the self-energies and spectral functions, we use the Matsubara Green's function technique [43]. We include the terms up to quadratic in the interaction \tilde{V} , which is the lowest order that gives nonzero contribution. The details of the derivation are given in Appendix B. In the final expression for retarded self-energy we replace the bare carrier Green's function with a dressed one, which constitutes the self-consistent Born approximation [43,44]. We thus obtain the following expression for retarded self-energy:

$$\Sigma_{\mathbf{k}}^R(\omega) = \Sigma_{\mathbf{k}}^{(1)}(\omega) + \Sigma_{\mathbf{k}}^{(2)}(\omega) + \Sigma_{\mathbf{k}}^{(3)}(\omega), \quad (21)$$

where

$$\begin{aligned} \Sigma_{\mathbf{k}}^{(1)}(\omega) &= \frac{1}{N_k \hbar^2} \sum_{\mathbf{q},f} |\phi_{\mathbf{q},f}|^2 [(n_f^{\text{ph}} + 1) G_{\mathbf{k}-\mathbf{q}}^R(\omega - \Omega_f) \\ &\quad + n_f^{\text{ph}} G_{\mathbf{k}-\mathbf{q}}^R(\omega + \Omega_f)], \end{aligned} \quad (22)$$

$$\begin{aligned} \Sigma_{\mathbf{k}}^{(2)}(\omega) &= \frac{-1}{N_k \hbar^2} \sum_{\mathbf{q},f} \phi_{\mathbf{q},f} \sum_{\mathbf{Y}} (D_{\mathbf{Y},f} - D_{\mathbf{X}+\mathbf{Y},f}) e^{i\mathbf{q}\cdot\mathbf{Y}} \\ &\quad \times \sum_{\mathbf{X}} J_{\mathbf{X}} \theta_{\mathbf{X}}^{(0)} [e^{i\mathbf{k}\cdot\mathbf{X}} - e^{-i(\mathbf{k}-\mathbf{q})\cdot\mathbf{X}}] [(n_f^{\text{ph}} + 1) \\ &\quad \times G_{\mathbf{k}-\mathbf{q}}^R(\omega - \Omega_f) - n_f^{\text{ph}} G_{\mathbf{k}-\mathbf{q}}^R(\omega + \Omega_f)], \end{aligned} \quad (23)$$

$$\begin{aligned} \Sigma_{\mathbf{k}}^{(3)}(\omega) &= \frac{1}{N_k \hbar^2} \sum_{\mathbf{q}} \sum_{\mathbf{X},\mathbf{Y},\mathbf{Z}} J_{\mathbf{X}} J_{\mathbf{Y}} \theta_{\mathbf{X}}^{(0)} \theta_{\mathbf{Y}}^{(0)} e^{i(\mathbf{k}-\mathbf{q})\cdot\mathbf{X}} e^{i\mathbf{k}\cdot\mathbf{Y}} \\ &\quad \times e^{i\mathbf{q}\cdot\mathbf{Z}} \int_{-\infty}^{\infty} dt e^{i\omega t} [\theta_{\mathbf{X},\mathbf{Y},\mathbf{Z}}(t) - 1] G_{\mathbf{k}-\mathbf{q}}^R(t). \end{aligned} \quad (24)$$

In these equations $G_{\mathbf{k}}^R(\omega)$ is the retarded self-energy, $\phi_{\mathbf{q},f}$ is defined as

$$\phi_{\mathbf{q},f} = G_f - \hbar \Omega_f \sum_{\mathbf{R}} D_{\mathbf{R},f} e^{-i\mathbf{q}\cdot\mathbf{R}}, \quad (25)$$

and

$$\begin{aligned} \theta_{\mathbf{X},\mathbf{Y},\mathbf{Z}}(t) &= \exp \left\{ - \sum_f [(n_f^{\text{ph}} + 1) e^{-i\Omega_f t} + n_f^{\text{ph}} e^{i\Omega_f t}] \right. \\ &\quad \left. \times \sum_{\mathbf{U}} (D_{\mathbf{U},f} - D_{\mathbf{U}+\mathbf{X},f}) (D_{\mathbf{U}+\mathbf{Z},f} - D_{\mathbf{U}+\mathbf{Z}+\mathbf{Y},f}) \right\}, \end{aligned} \quad (26)$$

while $G_{\mathbf{k}}^R(t)$ is the retarded Green's function in the time domain which is related to the Green's function in frequency domain as $G_{\mathbf{k}}^R(\omega) = \int_{-\infty}^{\infty} dt e^{i\omega t} G_{\mathbf{k}}^R(t)$. Retarded self-energies and Green's functions are then obtained by self-consistently solving the Dyson equation,

$$G_{\mathbf{k}}^R(\omega) = \frac{1}{\omega - \frac{E_{\mathbf{k}} - \mu_F}{\hbar} - \Sigma_{\mathbf{k}}^R(\omega)}, \quad (27)$$

and the equations for self-energies (21)–(24). In Eq. (27) the chemical potential is denoted as μ_F . The quantity $\phi_{\mathbf{q},f}$ can in some sense be considered as renormalized electron-phonon coupling. For all coupling strengths the minimization procedure yields $\phi_{\mathbf{q},f} = 0$ for $q = 0$. When electron-phonon coupling is small, $\phi_{\mathbf{q},f}$ is also small since both G_f and $D_{\mathbf{R},f}$ are small. For large electron-phonon coupling it is very small because in this case $D_{\mathbf{R},f} = \frac{G_f}{\hbar \Omega_f} \delta_{\mathbf{R},0}$; $\phi_{\mathbf{q},f}$ has the largest, but still relatively small, values for intermediate coupling strengths.

C. Mobility

The mobility in the direction i is given by the Kubo formula [40,43]

$$\mu_{ii} = \frac{\beta}{2N_c e_0} \int_{-\infty}^{\infty} dt \langle j_i^H(t) j_i \rangle_H, \quad (28)$$

where N_c is the total number of carriers in the system, e_0 is the elementary charge, while j_i is the i th component of the operator

$$\mathbf{j} = \frac{d\mathbf{P}}{dt}, \quad (29)$$

where \mathbf{P} is the polarization operator

$$\mathbf{P} = \sum_{\mathbf{R}} e_0 \mathbf{R} a_{\mathbf{R}}^{\dagger} a_{\mathbf{R}} \quad (30)$$

and the superscript H in the operator denotes the operators in the Heisenberg picture with respect to operator H ,

$$j_i^H(t) = e^{\frac{i}{\hbar}(H - \mu_F N)t} j_i e^{-\frac{i}{\hbar}(H - \mu_F N)t}, \quad (31)$$

where N is the particle number operator. Using $\frac{dP_i}{dt} = \frac{i}{\hbar} [H, P_i]$, we find

$$j_i = \sum_{\mathbf{k}} (\mathcal{J}_{\mathbf{k}})_i a_{\mathbf{k}}^{\dagger} a_{\mathbf{k}}, \quad (32)$$

where

$$(\mathcal{J}_k)_i = \frac{ie_0}{\hbar} \sum_{\mathbf{R}} J_{\mathbf{R}} \mathbf{R}_i e^{i\mathbf{k}\cdot\mathbf{R}}. \quad (33)$$

Next, we exploit the identity [45]

$$\langle j_i^H(t) j_i \rangle_H = \langle \tilde{j}_i^{\tilde{H}}(t) \tilde{j}_i \rangle_{\tilde{H}}, \quad (34)$$

where

$$\tilde{j}_i = U^{-1} j_i U = \frac{1}{N_k} \sum_{\mathbf{k}} (\mathcal{J}_k)_i \sum_{\mathbf{k}_1, \mathbf{k}_2} a_{\mathbf{k}_1}^\dagger a_{\mathbf{k}_2} \theta_{\mathbf{k}-\mathbf{k}_1}^\dagger \theta_{\mathbf{k}-\mathbf{k}_2} \quad (35)$$

and

$$\theta_{\mathbf{k}} = \frac{1}{\sqrt{N_k}} \sum_{\mathbf{R}} \theta_{\mathbf{R}} e^{i\mathbf{k}\cdot\mathbf{R}}. \quad (36)$$

From Eqs. (28), (34), and (35) we obtain

$$\begin{aligned} \mu_{ii} &= \frac{\beta}{2N_c e_0 N_k^2} \int_{-\infty}^{\infty} dt \sum_{\mathbf{k}, \mathbf{k}_0, \mathbf{k}_1, \mathbf{k}_2, \mathbf{k}_3, \mathbf{k}_4} (\mathcal{J}_k)_i (\mathcal{J}_{\mathbf{k}_0})_i \\ &\times \langle a_{\mathbf{k}_1}^{\tilde{H}}(t)^\dagger a_{\mathbf{k}_2}^{\tilde{H}}(t) a_{\mathbf{k}_3}^\dagger a_{\mathbf{k}_4} \theta_{\mathbf{k}-\mathbf{k}_1}^{\tilde{H}}(t)^\dagger \theta_{\mathbf{k}-\mathbf{k}_2}^{\tilde{H}}(t) \theta_{\mathbf{k}_0-\mathbf{k}_3}^\dagger \theta_{\mathbf{k}_0-\mathbf{k}_4} \rangle_{\tilde{H}}. \end{aligned} \quad (37)$$

To evaluate the mobility using Eq. (37), we will calculate the first nontrivial term in expansion of Eq. (37) in powers of interaction \tilde{V} . This is the zeroth term, which is obtained by replacing \tilde{H} by \tilde{H}_0 . Using the identity

$$\begin{aligned} \langle a_{\mathbf{k}_1}^{\tilde{H}_0}(t)^\dagger a_{\mathbf{k}_2}^{\tilde{H}_0}(t) a_{\mathbf{k}_3}^\dagger a_{\mathbf{k}_4} \rangle_{\tilde{H}_0} \\ = \langle a_{\mathbf{k}_1}^{\tilde{H}_0}(t)^\dagger a_{\mathbf{k}_4} \rangle_{\tilde{H}_0} \langle a_{\mathbf{k}_2}^{\tilde{H}_0}(t) a_{\mathbf{k}_3}^\dagger \rangle_{\tilde{H}_0} + \langle a_{\mathbf{k}_1}^{\tilde{H}_0}(t)^\dagger a_{\mathbf{k}_2}^{\tilde{H}_0}(t) \rangle_{\tilde{H}_0} \langle a_{\mathbf{k}_3}^\dagger a_{\mathbf{k}_4} \rangle_{\tilde{H}_0}, \end{aligned} \quad (38)$$

and omitting the second term which is proportional to the square of carrier population and is negligible in the limit of low carrier concentration that we consider here, we obtain

$$\mu_{ii} = \int_{-\infty}^{\infty} dt \mu'_{ii}(t), \quad (39)$$

where

$$\mu'_{ii}(t) = \frac{\beta}{2N_c e_0} \sum_{\mathbf{k}_1, \mathbf{k}_2} \langle a_{\mathbf{k}_1}(t)^\dagger a_{\mathbf{k}_1} \rangle \langle a_{\mathbf{k}_2}(t) a_{\mathbf{k}_2}^\dagger \rangle Y_{\mathbf{k}_1, \mathbf{k}_2}^{ii}(t), \quad (40)$$

$$\begin{aligned} Y_{\mathbf{k}_1, \mathbf{k}_2}^{ii}(t) &= \frac{1}{N_k^2} \sum_{\mathbf{k}, \mathbf{k}_0} (\mathcal{J}_k)_i (\mathcal{J}_{\mathbf{k}_0})_i \\ &\times \langle \theta_{\mathbf{k}-\mathbf{k}_1}^{\tilde{H}_0}(t)^\dagger \theta_{\mathbf{k}-\mathbf{k}_2}^{\tilde{H}_0}(t) \theta_{\mathbf{k}_0-\mathbf{k}_2}^\dagger \theta_{\mathbf{k}_0-\mathbf{k}_1} \rangle_{\tilde{H}_0} \\ &= -\frac{e_0^2}{\hbar^2 N_k} \sum_{\mathbf{X}, \mathbf{Y}, \mathbf{Z}} J_{\mathbf{X}} J_{\mathbf{Y}}(\mathbf{X})_i (\mathbf{Y})_i \\ &\times e^{i\mathbf{k}_1 \cdot (\mathbf{Y}+\mathbf{Z})} e^{i\mathbf{k}_2 \cdot (\mathbf{X}-\mathbf{Z})} \theta_{\mathbf{X}, \mathbf{Y}, \mathbf{Z}}(t) \theta_{\mathbf{X}}^{(0)} \theta_{\mathbf{Y}}^{(0)}, \end{aligned} \quad (41)$$

$$\langle a_{\mathbf{k}_1}(t)^\dagger a_{\mathbf{k}_1} \rangle = \frac{1}{2\pi} \int_{-\infty}^{\infty} d\omega e^{i\omega t} \frac{A_{\mathbf{k}_1}(\omega)}{1 + e^{\beta\hbar\omega}}, \quad (42)$$

$$\langle a_{\mathbf{k}_2}(t) a_{\mathbf{k}_2}^\dagger \rangle = \frac{1}{2\pi} \int_{-\infty}^{\infty} d\omega e^{-i\omega t} A_{\mathbf{k}_2}(\omega). \quad (43)$$

In Eqs. (42) and (43) we have replaced the bare spectral function $A_{\mathbf{k}}^{(0)}(\omega) = -2\text{Im}G_{\mathbf{k}}^{(0),R}(\omega)$ [where $G_{\mathbf{k}}^{(0),R}(\omega)$ denotes the retarded Green's function for \tilde{H}_0] with a dressed one $A_{\mathbf{k}}(\omega) = -2\text{Im}G_{\mathbf{k}}^R(\omega)$ in the spirit of the self-consistent Born approximation which was used to calculate the retarded Green's functions and self-energies. This replacement is equivalent to taking the zeroth term in the expansion of mobility in terms of dressed Green's function. It leads to time decay of the current-current correlation function and is essential to obtain finite values of mobility. It can be, in principle, further systematically improved by adding higher-order diagrams in the expansion, such as the vertex corrections [43].

III. RESULTS—ONE DIMENSIONAL HOLSTEIN MODEL

To illustrate the application of the whole approach, we consider a one-dimensional system, with electronic coupling between nearest neighbors only and with a single-phonon mode per lattice site, which constitutes the well-known Holstein model [13]. The system is described by the following parameters: the transfer integral J , the phonon energy $\hbar\Omega$, the electron-phonon coupling strength G , and the thermal energy $k_B T$.

A. Numerical aspects

The calculations of Green's functions, spectral functions, and self-energies were performed by self-consistently solving the Dyson equation [Eq. (27)] and the equations for self-energies (21)–(24). Namely, we start with an initial guess $\Sigma_{\mathbf{k}}(\omega) = -iJ/5$ and then we evaluate the Green's function using Eq. (27). Next, we evaluate new self-energy using Eqs. (21)–(24). The $\Sigma_{\mathbf{k}}^{(1)}(\omega)$ and $\Sigma_{\mathbf{k}}^{(2)}(\omega)$ are evaluated in the frequency domain, while $\Sigma_{\mathbf{k}}^{(3)}(t)$ is evaluated in the time domain and then converted to frequency domain. Self-energies and Green's functions were represented on a uniform grid of k and ω points. Typical size of the uniform k -point grid was 90, while typical size of the uniform grid used to represent the frequency and time dependence was 10 000–20 000 and the frequency range was from $(-20\frac{J}{\hbar}, 20\frac{J}{\hbar})$ to $(-120\frac{J}{\hbar}, 120\frac{J}{\hbar})$, depending on the parameters of the system. Evaluated self-energy is then mixed in a 50–50% ratio with a self-energy from previous iteration to ensure convergence of the whole process. The process is stopped when self-energy from current iteration becomes nearly the same as self-energy from previous iteration. Typical computational time on a single computer for a given set of system parameters and for reported grid dimensions is on the order of tens of minutes. We note that in many cases the grid size can be significantly reduced without compromising accuracy and that computational times on the order of minutes can be reached. Further speed-up of calculations could be in principle achieved by representing the self-energies in real space and exploiting their locality. On the other hand, straightforward numerical evaluation using uniform grid representations becomes rather challenging at low temperatures when linewidth of the spectral function becomes very narrow. For this reason, we also derive analytical expressions for limiting behavior of spectral functions and mobility in this region.

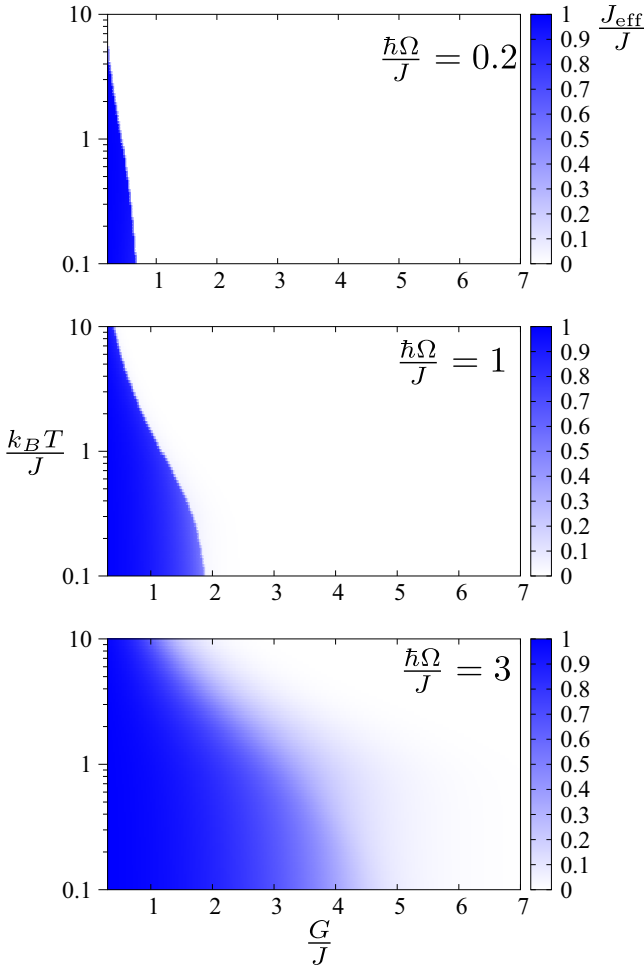


FIG. 1. Dependence of band dispersion narrowing factor $\frac{J_{\text{eff}}}{J}$ on electron-phonon coupling strength $\frac{G}{J}$ and temperature $\frac{k_B T}{J}$ for different values of phonon energies $\frac{\hbar\Omega}{J}$.

B. Band dispersion narrowing and spectral functions

First, we analyze the values of optimal parameters of the unitary transformation. The parameter $\theta_{a_l}^{(0)}$ defined in Eq. (12) (where a_l is the lattice constant) is the ratio $\frac{J_{\text{eff}}}{J}$ of the band dispersion widths of noninteracting part of the transformed and original Hamiltonian, as can be seen from Eq. (10). For brevity, it can be called the band dispersion narrowing factor and its value gives a good indication of the transport regime. In Fig. 1 we present its dependence on electron-phonon interaction strength $\frac{G}{J}$ and temperature $\frac{k_B T}{J}$ for different values of phonon energies $\frac{\hbar\Omega}{J} = 0.2$, $\frac{\hbar\Omega}{J} = 1$, and $\frac{\hbar\Omega}{J} = 3$. From Fig. 1 we see that for all phonon energies $\frac{\hbar\Omega}{J}$ the band dispersion narrowing factor exhibits values close to 1 at low temperatures and small electron-phonon coupling constants, while it exhibits values close to zero at high temperatures and large electron-phonon coupling constants. In the regime of low temperature and small electron-phonon coupling the parameters of the unitary transformation are also close to zero $D_n \approx 0$ (where n is an integer that labels the lattice site). On the other hand, in the opposite regime of high temperatures and large electron-phonon coupling constants optimal parameters of the transformation read $D_m \approx \frac{G}{\hbar\Omega} \delta_{m,0}$. In case of small ($\frac{\hbar\Omega}{J} = 0.2$)

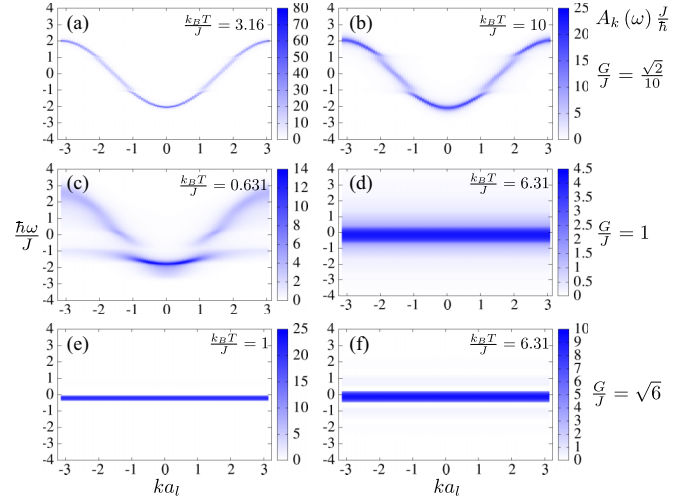


FIG. 2. Spectral function at phonon energy of $\frac{\hbar\Omega}{J} = 1$ and different values of electron-phonon coupling strength $\frac{G}{J}$ and temperature $\frac{k_B T}{J}$: (a) $\frac{k_B T}{J} = 3.16$, $\frac{G}{J} = \frac{\sqrt{2}}{10}$; (b) $\frac{k_B T}{J} = 10$, $\frac{G}{J} = \frac{\sqrt{2}}{10}$; (c) $\frac{k_B T}{J} = 0.631$, $\frac{G}{J} = 1$; (d) $\frac{k_B T}{J} = 6.31$, $\frac{G}{J} = 1$; (e) $\frac{k_B T}{J} = 1$, $\frac{G}{J} = \sqrt{6}$; (f) $\frac{k_B T}{J} = 6.31$, $\frac{G}{J} = \sqrt{6}$.

and medium ($\frac{\hbar\Omega}{J} = 1$) phonon energies the change in the band dispersion narrowing factor at the transition between the two regimes is abrupt, while in the case of large phonon energies ($\frac{\hbar\Omega}{J} = 3$), this change is rather smooth (see Fig. 1). We note for the moment that abruptness of this transition is an undesirable feature of unitary transformation and that no physical meaning (such as, for example, the phase transition) should be associated to smoothness or abruptness of this transition. We leave the discussion of its implications for the part with presentation of mobility results. It has been well established (see, for example, Refs. [17,46]) that the crossover from the regime of free carriers to the small-polaron regime is smooth and at zero temperature occurs when both conditions $\lambda > 1$ and $\alpha^2 > 1$ are satisfied, where $\lambda = \frac{G^2}{2J\hbar\Omega}$ and $\alpha = \frac{G}{\hbar\Omega}$. These two conditions are fulfilled if $\lambda > 1$ when $\frac{\hbar\Omega}{J}$ is small (adiabatic regime), while they are fulfilled if $\alpha^2 > 1$ when $\frac{\hbar\Omega}{J}$ is large (anadiabatic regime). The crossover between the dark and white regions at low temperature in Fig. 1 indeed occurs at coupling strength when these conditions are satisfied.

For presentation of the results, we chose the transfer integral J as the energy unit and not the phonon energy $\hbar\Omega$ which is a somewhat more conventional choice in the literature. Our choice was motivated by the fact that this enables us to establish the effect of phonon energy on band dispersion narrowing. While it is well established that larger electron-phonon interaction and higher temperature narrow the band dispersion and larger transfer integral widens the band, it is not clear what is the effect of phonon energy. From Fig. 1, we see that larger phonon energy also leads to band dispersion widening.

Since spectral function $A_k(\omega)$ is one of the key factors that determines the mobility [Eqs. (39)–(43)], we analyze it in more detail as follows. In Fig. 2 we present the spectral function at intermediate values of phonon energy $\frac{\hbar\Omega}{J} = 1$

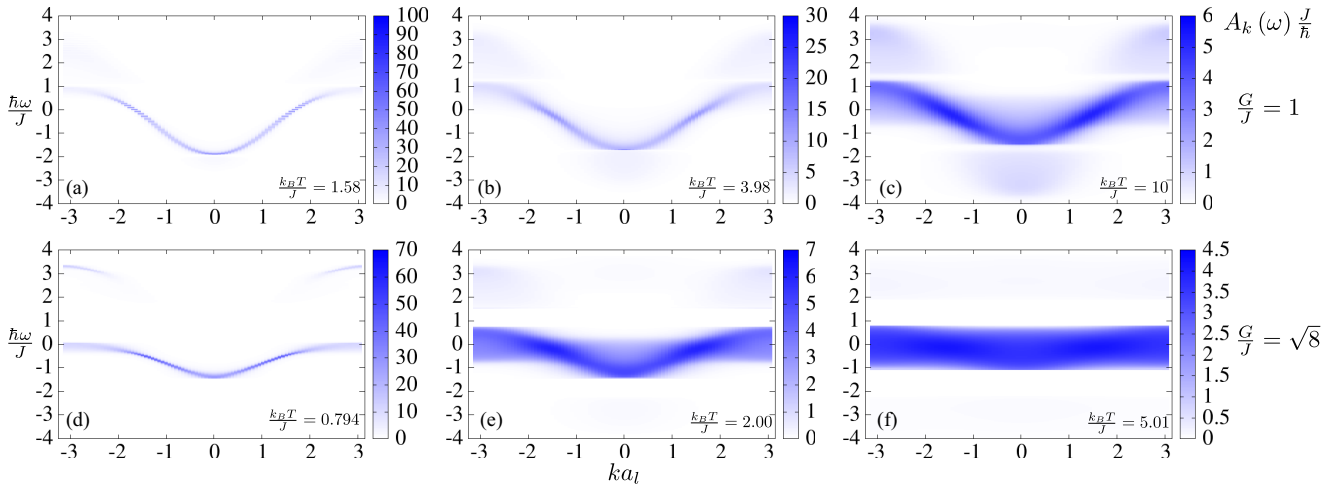


FIG. 3. Spectral function at phonon energy of $\frac{\hbar\Omega}{J} = 3$ and different values of electron-phonon coupling strength $\frac{G}{J}$ and temperature $\frac{k_B T}{J}$: (a) $\frac{k_B T}{J} = 1.58$, $\frac{G}{J} = 1$; (b) $\frac{k_B T}{J} = 3.98$, $\frac{G}{J} = 1$; (c) $\frac{k_B T}{J} = 10$, $\frac{G}{J} = 1$; (d) $\frac{k_B T}{J} = 0.794$, $\frac{G}{J} = \sqrt{8}$; (e) $\frac{k_B T}{J} = 2.00$, $\frac{G}{J} = \sqrt{8}$; (f) $\frac{k_B T}{J} = 5.01$, $\frac{G}{J} = \sqrt{8}$.

for different values of electron-phonon coupling strength and temperature. At low values of electron-phonon coupling and temperature [see Fig. 2(a)] the shape of spectral function plot is fully determined by the bare band dispersion and the linewidth of the spectral function is narrow. As the temperature increases, the linewidth becomes broader [see Fig. 2(b)] and slight band splitting at the energy $\hbar\Omega$ above the band minimum appears. At intermediate electron-phonon coupling strengths the spectral function at low temperatures [see Fig. 2(c)] still exhibits a pronounced dispersion but with stronger broadening and band splitting. After a certain temperature when an abrupt change in parameters of the unitary transformation takes place, the dispersion becomes flat [see Fig. 2(d)] and momentum dependence of the spectral function is lost. At high values of electron-phonon coupling the dispersion remains flat, while an increase in temperature broadens the linewidth [see Figs. 2(e) and 2(f)]. The spectral function at low values of phonon energy $\frac{\hbar\Omega}{J} = 0.2$ exhibits qualitatively the same behavior as for intermediate values. At high values of phonon energy we also find that an increase of temperature broadens the linewidth and narrows the bands [see Figs. 3(a)–3(f)]. A qualitative difference in this case compared with low and intermediate values of phonon energy is that the spectral function evolves smoothly from a dispersive and narrow linewidth form to a flat and broad linewidth form [see, e.g., Figs. 3(d)–3(f)] without an abrupt change of its shape.

C. Carrier mobility

In Fig. 4 we present temperature dependence of mobility for different electron-phonon coupling strengths and phonon energies. For each phonon energy, the calculations were performed for electron-phonon interaction strengths ranging from small values where electron-phonon interaction is merely a perturbation to large values significantly after the crossover to the small-polaron regime. In the following, we discuss these results in detail.

1. Weak electron-phonon coupling

At low values of electron-phonon coupling for each $\frac{\hbar\Omega}{J}$ we find that the mobility decreases with an increase in temperature. To better understand the origin of such a dependence, we first derive the expression for mobility in the limit of small electron-phonon coupling. In this case, the parameters of unitary transformation are approximately zero: $D_{\mathbf{R},f} \approx 0$. The $\theta_{\mathbf{R}}$ operators [Eq. (17)] then take the form of unity operators $\theta_{\mathbf{R}} \approx 1$, which leads to $\theta_{\mathbf{k}} \approx \sqrt{N_k} \delta_{\mathbf{k},0}$ [where $\theta_{\mathbf{k}}$ was defined in Eq. (36)]. From Eq. (41) we then obtain $Y_{\mathbf{k}_1, \mathbf{k}_2}^{ii}(t) \approx (\mathcal{J}_{\mathbf{k}_1})_i (\mathcal{J}_{\mathbf{k}_2})_i \delta_{\mathbf{k}_1, \mathbf{k}_2}$. Using Eqs. (39), (40), (42), and (43) we come to the expression

$$\mu = \frac{\beta}{2N_c e_0} \sum_{\mathbf{k}} \mathcal{J}_{\mathbf{k}}^2 \frac{1}{2\pi} \int d\omega A_{\mathbf{k}}(\omega)^2 n_F(\omega), \quad (44)$$

where $n_F(\omega) = \frac{1}{e^{\beta\hbar\omega} + 1}$. Next we exploit the identity

$$A_{\mathbf{k}}(\omega)^2 = 2\pi \frac{\delta[\omega - \frac{E_{\mathbf{k}} - \mu_F}{\hbar}]}{-\text{Im}\Sigma_{\mathbf{k}}^R(\omega)}, \quad (45)$$

which is valid in the limit of small self-energy and obtain

$$\mu = \frac{\beta}{e_0} \frac{\sum_{\mathbf{k}} n_{\mathbf{k}} \tau_{\mathbf{k}} \mathcal{J}_{\mathbf{k}}^2}{\sum_{\mathbf{k}} n_{\mathbf{k}}}, \quad (46)$$

where $n_{\mathbf{k}} = \frac{1}{e^{\beta(E_{\mathbf{k}} - \mu_F)} + 1}$ and

$$\frac{1}{\tau_{\mathbf{k}}} = -2\text{Im}\Sigma_{\mathbf{k}}(\omega)|_{\omega = \frac{E_{\mathbf{k}} - \mu_F}{\hbar}}. \quad (47)$$

We further exploit the fact that $D_{\mathbf{R},f} \approx 0$ implies that $\Sigma_{\mathbf{k}}^{(2)}$ and $\Sigma_{\mathbf{k}}^{(3)}$ terms [see Eqs. (23) and (24)] vanish. The $\phi_{\mathbf{q},f}$ term in Eq. (25) reduces to $\phi_{\mathbf{q},f} = G_f$. Using Eq. (22) we obtain in this limit

$$\frac{1}{\tau_{\mathbf{k}}} = \frac{2\pi}{\hbar} \frac{1}{N_k} \sum_{\mathbf{q},f} G_f^2 [(n_f^{\text{ph}} + 1) \delta(E_{\mathbf{k}} - \hbar\Omega_f - E_{\mathbf{k}-\mathbf{q}}) + n_f^{\text{ph}} \delta(E_{\mathbf{k}} + \hbar\Omega_f - E_{\mathbf{k}-\mathbf{q}})]. \quad (48)$$

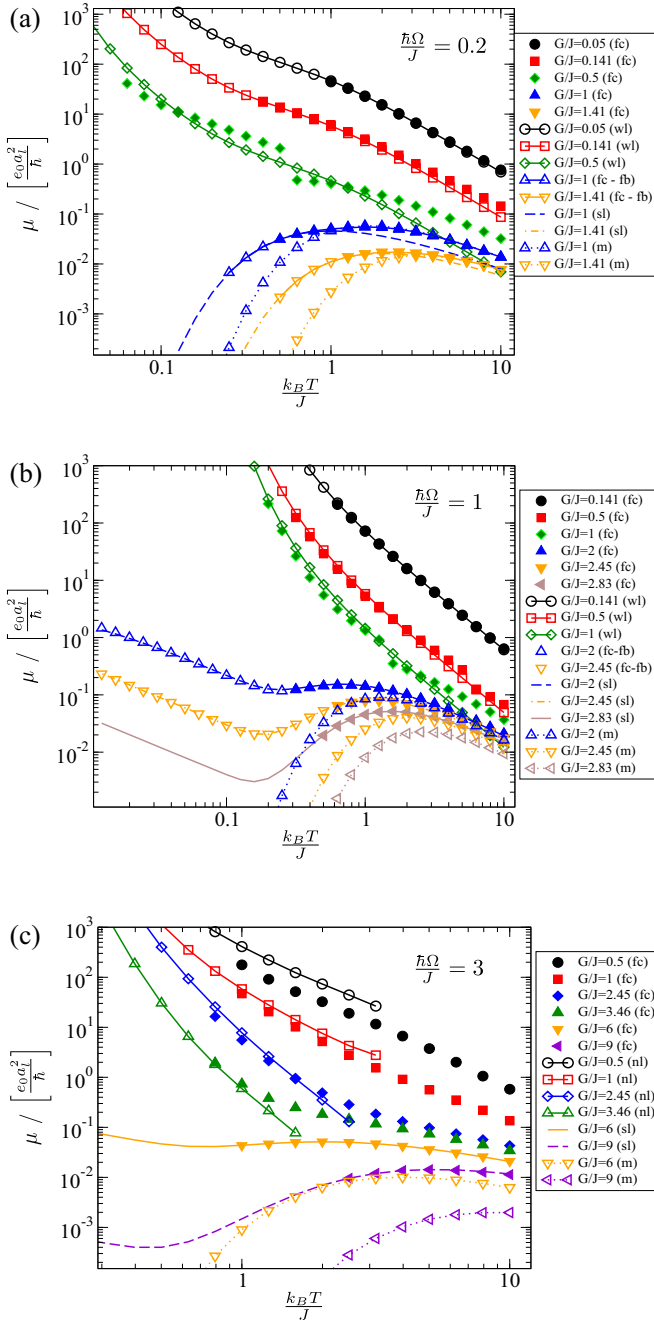


FIG. 4. Temperature dependence of mobility for different electron-phonon coupling strengths $\frac{G}{J}$ and phonon energies: (a) $\frac{\hbar\Omega}{J} = 0.2$, (b) $\frac{\hbar\Omega}{J} = 1$, and (c) $\frac{\hbar\Omega}{J} = 3$. The label “fc” denotes full calculation using the spectral function obtained from the self-consistent solution of Eqs. (21)–(24) and (27) and mobility obtained from Eqs. (39)–(43). The label “wl” denotes the weak electron-phonon coupling limit results obtained from Eq. (49). The label “fc-fb” denotes full calculation where momentum dependence of Green’s functions and self-energies was neglected, i.e., Eqs. (53), (54), (56), and (27) were used. The label “sl” denotes the strong electron-phonon coupling limit results obtained from Eq. (65). The label “nl” denotes the mobility obtained using the narrow linewidth approximation with spectral function obtained from Eqs. (70) and (69) and the mobility calculated as described in Appendix D. The label “m” denotes the mobility obtained using the Marcus formula from Eqs. (75) and (76).

Equations (48) and (46) are exactly the equations that one would obtain by perturbative treatment of electron-phonon interaction from the beginning without resorting to the use of unitary transformation. The fact that these equations were also obtained from our approach in the limit of small electron-phonon interaction is a good validity check of our approach. The two terms in square brackets in Eq. (48) originate respectively from scattering of carrier with momentum \mathbf{k} due to emission and absorption of phonons. We further note that the time given by Eq. (48) is the carrier scattering time rather than the momentum relaxation time [given by Eq. (C9)] that would be obtained if vertex corrections were included [43]. It is interesting to note that in the case of one-dimensional Holstein model these two times are the same, as shown in Appendix C.

In the case of Holstein model, Eqs. (48) and (46) can be further integrated, as described in detail in Appendix C. The final result for mobility in this limit then reads

$$\begin{aligned} \mu = & \frac{e_0 a_1^2}{\hbar} \frac{4\beta J^3}{\pi G^2 I_0(2\beta J)} \\ & \times \left[\frac{1}{n^{\text{ph}}} \int_0^{k_A a_1} du e^{2\beta J \cos u} \sin^2 u \sqrt{1 - \left(\cos u - \frac{\hbar\Omega}{2J} \right)^2} \right. \\ & + \int_{k_A a_1}^{k_B a_1} \frac{du e^{2\beta J \cos u} \sin^2 u}{\frac{n^{\text{ph}}}{\sqrt{1 - \left(\cos u - \frac{\hbar\Omega}{2J} \right)^2}} + \frac{n^{\text{ph}+1}}{\sqrt{1 - \left(\cos u + \frac{\hbar\Omega}{2J} \right)^2}}} \\ & \left. + \frac{1}{n^{\text{ph}+1}} \int_{k_B a_1}^{\pi} du e^{2\beta J \cos u} \sin^2 u \sqrt{1 - \left(\cos u + \frac{\hbar\Omega}{2J} \right)^2} \right], \end{aligned} \quad (49)$$

where $k_A = \frac{1}{a_1} \arccos(1 - \frac{\hbar\Omega}{2J})$, $k_B = \frac{\pi}{a_1} - \frac{1}{a_1} \arccos(1 - \frac{\hbar\Omega}{2J})$, and $I_n(x)$ denotes the modified Bessel function of the first kind of order n . In Figs. 4(a) and 4(b) we present the temperature dependence of the mobility calculated using Eq. (49) [the lines labeled as “wl” (weak limit)]. When $\frac{\hbar\Omega}{J} = 0.2$ the weak limit results agree perfectly with full calculation for smallest investigated strength of electron-phonon interaction $\frac{G}{J} = 0.05$ [see Fig. 4(a)]. The agreement is also excellent for $\frac{G}{J} = 0.1\sqrt{2}$ except for largest temperatures where the effects of electron-phonon interaction become stronger due to larger number of phonons, while the agreement gets significantly worse at $\frac{G}{J} = 0.5$. For medium phonon energies $\frac{\hbar\Omega}{J} = 1$, we also obtain excellent agreement of the weak limit result with full calculation at lowest electron-phonon interaction strength of $\frac{G}{J} = 0.1\sqrt{2}$ and at lower temperatures for $\frac{G}{J} = 0.5$ and 1 [see Fig. 4(b)].

Equation (49) is also important as it provides the opportunity to calculate the mobility at lower temperatures when linewidth of the spectral function becomes very narrow. It is then more difficult to perform full calculation since a very dense frequency grid is needed to represent the Green’s functions.

It is important to note that Eq. (49) should be applied only when $\frac{\hbar\Omega}{J} < 2$. In the opposite case, there exist k points for which electron scattering via phonon emission or absorption

is not possible because final state energy is outside the range of band energies. For these k points, the scattering time calculated using Eq. (48) is infinite, as well as the mobility obtained using Eq. (49). For this reason, it is not possible to present the mobility obtained from Eq. (49) in Fig. 4(c) when $\frac{\hbar\Omega}{J} = 3$.

2. Strong electron-phonon coupling

Next we discuss the temperature dependence of the mobility for large values of electron-phonon interaction. From the results presented in Fig. 4, we see that this dependence exhibits rich features that depend on phonon energy $\frac{\hbar\Omega}{J}$. For $\frac{\hbar\Omega}{J} = 0.2$ the mobility exhibits a maximum at certain temperature followed by a decrease as the temperature further increases. On the other hand, for $\frac{\hbar\Omega}{J} = 1$ and 3 one minimum followed by one maximum appear in the dependence.

To better understand these dependencies and the origin of the differences between them, we have derived analytical formulas in the limit of strong electron-phonon interaction. In this limit, the parameters of the unitary transformation take the form $D_{\mathbf{R},f} = \frac{G_f}{\hbar\Omega_f} \delta_{\mathbf{R},0}$ and these are sufficiently large that band dispersion narrowing factor $\theta_{a_i}^{(0)}$ is approximately zero. As a consequence of strong band dispersion narrowing, all momentum dependencies in the self-energy and Green's functions are lost [see, e.g., the spectral function in Fig. 2(e)] and we can consider them to be a function of ω only. The term $\phi_{\mathbf{q},f}$ [Eq. (25)] also becomes zero since $D_{\mathbf{R},f} = \frac{G_f}{\hbar\Omega_f} \delta_{\mathbf{R},0}$ in this limit. Consequently, the terms $\Sigma_{\mathbf{k}}^{(1)}(\omega)$ [Eq. (22)] and $\Sigma_{\mathbf{k}}^{(2)}(\omega)$ [Eq. (23)] also vanish in this limit and self-energy is determined by the $\Sigma_{\mathbf{k}}^{(3)}(\omega)$ term [Eq. (24)].

By neglecting the momentum dependence of the Green's function in Eq. (24) and exploiting the identity $\frac{1}{N_k} \sum_{\mathbf{q}} e^{i\mathbf{q}\cdot(\mathbf{Z}-\mathbf{X})} = \delta_{\mathbf{X},\mathbf{Z}}$ we obtain

$$\begin{aligned} \Sigma_{\mathbf{k}}^R(\omega) &= \frac{1}{\hbar^2} \sum_{\mathbf{X},\mathbf{Y}} J_{\mathbf{X}} J_{\mathbf{Y}} \theta_{\mathbf{X}}^{(0)} \theta_{\mathbf{Y}}^{(0)} e^{i\mathbf{k}\cdot(\mathbf{X}+\mathbf{Y})} \\ &\times \int_{-\infty}^{\infty} dt e^{i\omega t} [\theta_{\mathbf{X},\mathbf{Y},\mathbf{X}}(t) - 1] G^R(t). \end{aligned} \quad (50)$$

The term $\theta_{\mathbf{X},\mathbf{Y},\mathbf{X}}(t)$ in this limit reads

$$\begin{aligned} \theta_{\mathbf{X},\mathbf{Y},\mathbf{X}}(t) &= \exp \left\{ - \sum_f [(n_f^{\text{ph}} + 1) e^{-i\Omega_f t} + n_f^{\text{ph}} e^{i\Omega_f t}] \right. \\ &\times \left(\frac{G_f}{\hbar\Omega_f} \right)^2 \sum_{\mathbf{U}} (\delta_{\mathbf{U},0} \delta_{\mathbf{X},0} - \delta_{\mathbf{U},0} \delta_{\mathbf{X}+\mathbf{Y},0} \\ &\left. - \delta_{\mathbf{U}+\mathbf{X},0} + \delta_{\mathbf{U}+\mathbf{X},0} \delta_{\mathbf{Y},0}) \right\}. \end{aligned} \quad (51)$$

After omitting the terms $\delta_{\mathbf{X},0}$ and $\delta_{\mathbf{Y},0}$ which do not contribute since these are nonzero only when $J_{\mathbf{X}}$ or $J_{\mathbf{Y}}$ are zero, we obtain

$$\theta_{\mathbf{X},\mathbf{Y},\mathbf{X}}(t) = e^{\sum_f [(n_f^{\text{ph}}+1)e^{-i\Omega_f t} + n_f^{\text{ph}} e^{i\Omega_f t}] \left(\frac{G_f}{\hbar\Omega_f}\right)^2 (1+\delta_{\mathbf{X}+\mathbf{Y},0})}. \quad (52)$$

In the strong electron-phonon coupling limit, the dominant term is obtained when $\delta_{\mathbf{X}+\mathbf{Y},0} = 1$, i.e., $\mathbf{X} = -\mathbf{Y}$. After

including this term only, we come to the expression

$$\Sigma^R(\omega) = \frac{1}{\hbar^2} \sum_{\mathbf{X}} J_{\mathbf{X}}^2 [\theta_{\mathbf{X}}^{(0)}]^2 \int_{-\infty}^{\infty} dt e^{i\omega t} \theta_{\mathbf{X},-\mathbf{X},\mathbf{X}}(t) G^R(t), \quad (53)$$

with

$$\theta_{\mathbf{X},-\mathbf{X},\mathbf{X}}(t) = e^{2\sum_f [(n_f^{\text{ph}}+1)e^{-i\Omega_f t} + n_f^{\text{ph}} e^{i\Omega_f t}] \left(\frac{G_f}{\hbar\Omega_f}\right)^2}. \quad (54)$$

Using Eqs. (39)–(41) we find

$$\begin{aligned} \mu_{ii} &= \frac{-\beta e_0}{2N_c \hbar^2 N_k} \int_{-\infty}^{\infty} dt \sum_{\mathbf{k}_1, \mathbf{k}_2} \langle a(t)^\dagger a \rangle \langle a(t) a^\dagger \rangle \\ &\times \sum_{\mathbf{X}, \mathbf{Y}, \mathbf{Z}} J_{\mathbf{X}} J_{\mathbf{Y}} (\mathbf{X})_i (\mathbf{Y})_i e^{i\mathbf{k}_1 \cdot (\mathbf{Y}+\mathbf{Z})} e^{i\mathbf{k}_2 \cdot (\mathbf{X}-\mathbf{Z})} \\ &\times \theta_{\mathbf{X},\mathbf{Y},\mathbf{Z}}(t) \theta_{\mathbf{X}}^{(0)} \theta_{\mathbf{Y}}^{(0)}, \end{aligned} \quad (55)$$

where momentum dependence in the expectation values of products of fermionic operators was neglected. Using the identities $\frac{1}{N_k} \sum_{\mathbf{k}_1} e^{i\mathbf{k}_1 \cdot (\mathbf{Y}+\mathbf{Z})} = \delta_{\mathbf{Y},-\mathbf{Z}}$ and $\frac{1}{N_k} \sum_{\mathbf{k}_2} e^{i\mathbf{k}_2 \cdot (\mathbf{X}-\mathbf{Z})} = \delta_{\mathbf{X},\mathbf{Z}}$ we find

$$\begin{aligned} \mu_{ii} &= \frac{\beta e_0 N_k}{2N_c \hbar^2} \int_{-\infty}^{\infty} dt \sum_{\mathbf{X}} J_{\mathbf{X}}^2 (\mathbf{X})_i^2 [\theta_{\mathbf{X}}^{(0)}]^2 \theta_{\mathbf{X},-\mathbf{X},\mathbf{X}}(t) \\ &\times \langle a(t)^\dagger a \rangle \langle a(t) a^\dagger \rangle. \end{aligned} \quad (56)$$

The connection of this expression with known small-polaron hopping and Marcus formulas will be discussed in Sec. IV. Further simplifications of Eq. (56) are possible in the case of the Holstein model. Equation (53) then takes the form

$$\Sigma^R(t) = \frac{2J^2}{\hbar^2} \Theta(t) G^R(t), \quad (57)$$

where

$$\Theta(t) = [\theta_{a_i}^{(0)}]^2 \theta_{a_i, -a_i, a_i}(t). \quad (58)$$

In the presence of a single-phonon mode, the function $\Theta(t)$ is periodic with period $\frac{2\pi}{\Omega}$ and can be expressed in terms of the Fourier series as

$$\Theta(t) = \sum_n \Theta_n e^{in\Omega t} \quad (59)$$

with

$$\Theta_n = \frac{\Omega}{2\pi} \int_{-\pi/\Omega}^{\pi/\Omega} dt \Theta(t) e^{-in\Omega t}. \quad (60)$$

Equation (57) then takes the form

$$\Sigma^R(\omega) = \frac{2J^2}{\hbar^2} \sum_n \Theta_n G^R(\omega + n\Omega). \quad (61)$$

When the linewidth of the spectral function becomes narrow, i.e., when it is significantly smaller than Ω it is only the $n = 0$ term that gives a significant contribution in the last expression. Consequently, from equations $\Sigma^R(\omega) = \frac{2J^2}{\hbar^2} \Theta_0 G^R(\omega)$ and the Dyson equation $G^R(\omega) = \frac{1}{\omega - \Sigma^R(\omega)}$ one finds

$$A(\omega) = -2\text{Im}G^R(\omega) = \begin{cases} 0 & \text{if } |\omega| > 2\sqrt{a_t} \\ \sqrt{4a_t - \omega^2} & \text{if } |\omega| \leq 2\sqrt{a_t} \end{cases}, \quad (62)$$

where

$$a_t = \frac{2J^2}{\hbar^2} \Theta_0. \quad (63)$$

From Eqs. (56), (58), (59), (42), and (43) we obtain

$$\mu = \frac{\beta N_k e_0 J^2 a_l^2}{2\pi N_c \hbar^2} \sum_n \Theta_n \int_{-\infty}^{\infty} d\omega n_F(\omega) A(\omega) A(\omega + n\Omega). \quad (64)$$

When the linewidth of the spectral function is significantly narrower than Ω , the product of the spectral functions in the last expression has significant values only when $n = 0$. By including this term only, using Eq. (62), and performing the frequency integration, we come to the expression

$$\mu = 2 \frac{e_0 a_l^2}{\hbar} \frac{\gamma \cosh \gamma - \sinh \gamma}{\pi \gamma I_1(\gamma)}, \quad (65)$$

where $\gamma = 2\beta J \sqrt{2\Theta_0}$. Equation (65) can be further simplified when $\gamma \ll 1$ to

$$\mu = \frac{4}{3\pi} \frac{e_0 a_l^2}{\hbar} \gamma. \quad (66)$$

In addition to the results of the full simulation, in Fig. 4 we also present the following results: (i) The mobility obtained using Eq. (56) with self-energy from Eq. (53), which will be denoted as fc-fb (full calculation with flat bands) and (ii) the mobility obtained using analytical formula from Eq. (65), which will be denoted as sl (strong limit). As can be seen from Fig. 4 for large electron-phonon interaction strengths [$\frac{G}{J} \geq 1$ in Fig. 4(a), $\frac{G}{J} \geq 2$ in Fig. 4(b), and $\frac{G}{J} \geq 5$ in Fig. 4(c)] the results of the calculation with flat bands fully agree with the results of the full calculation for parameters where full calculation can be performed. This is expected since momentum dependence of the spectral functions is lost in this range of parameters [see, e.g., Figs. 2(e) and 2(f)]. On the other hand, the results obtained using Eq. (65) also agree excellently with the results of full calculation [see Figs. 4(a)–4(c)] except for highest temperatures in Fig. 4(a). At these high temperatures, the condition that spectral linewidth is narrower than the phonon frequency becomes violated. Since Eq. (65) is analytical and for most parameter values when electron-phonon interaction is strong it excellently reproduces the results of full calculation, it can be analyzed to gain insight into the origin of obtained temperature dependencies.

For all the data labeled as sl and presented in Fig. 4 the condition $\gamma \ll 1$ is satisfied and therefore it follows from Eq. (66) that the mobility is then determined by the product of the $\sqrt{\Theta_0}$ term and the inverse temperature. The $\sqrt{\Theta_0}$ term is in this range of parameters proportional to the linewidth of the spectral function [as follows from Eqs. (62) and (63)]. As a consequence, the following interpretation can be given to the mobility expression. As the temperature increases, the residual polaron-phonon interaction broadens the linewidth and consequently increases the diffusivity. The inverse temperature in the mobility expression arises due to the relation between mobility and diffusion constant. The dependence of the Θ_0 factor on temperature is presented in Fig. 5. For $\frac{\hbar\Omega}{J} = 1$ the graph of the dependence of Θ_0 on temperature can be divided into three parts. This term is constant (and equal to its

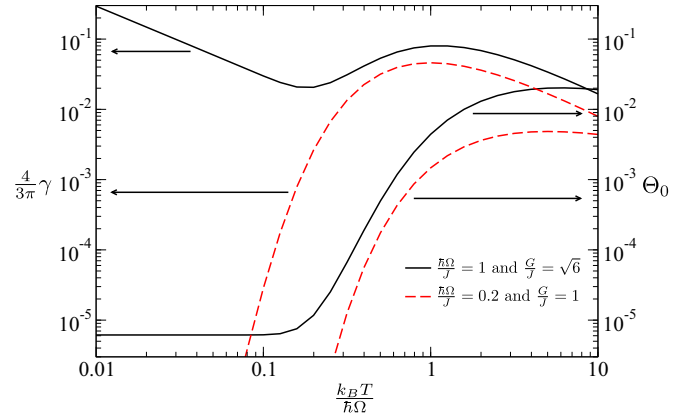


FIG. 5. Temperature dependence of the γ and the Θ_0 term that determine the mobility for $\frac{\hbar\Omega}{J} = 1$ and $\frac{G}{J} = \sqrt{6}$ (solid line), as well as for $\frac{\hbar\Omega}{J} = 0.2$ and $\frac{G}{J} = 1$ (dashed line).

zero temperature limit) at low temperatures and then sharply increases as the temperature increases (due to exponential rise in the number of phonons) and again becomes nearly constant at high temperatures (when the number of phonons is close to reaching its classical limit). The first part of this dependence then leads to $\sim \frac{1}{T}$ dependence of mobility at low temperatures, the second part to an increase of mobility at medium temperatures, and the third part leads again to a decreasing mobility at high temperatures. On the other hand, for $\frac{\hbar\Omega}{J} = 0.2$ the temperature at which Θ_0 reaches the zero-temperature limit is extremely low (below the temperatures presented in the figures) and therefore the graph of the dependence of Θ_0 on temperature consists of two parts—in the first part it sharply increases as the temperature increases and then becomes nearly constant. The first part of this dependence leads to an increase of mobility as the temperature increases, while the second part leads to a mobility that decreases.

3. Intermediate values of electron-phonon coupling

In this subsection, we discuss the results obtained for intermediate values of electron-phonon coupling and small and intermediate values of phonon energy, such as the results presented in Fig. 4(a) for $\frac{G}{J} = 0.5$ and the results in Fig. 4(b) for $\frac{G}{J} = 1$. At these electron-phonon coupling strengths, there exists a temperature where a sudden change of parameters of optimal unitary transformation occurs. At this temperature, calculated temperature dependence of mobility ceases to be continuous and the mobility exhibits a slight drop as the temperature increases, see Figs. 4(a) and 4(b). On the other hand, it has been well established that the Holstein model does not exhibit a phase transition and, consequently, the temperature dependence of physical observables such as the mobility should be smooth [47]. The discontinuity obtained in the calculation is therefore an artifact of our variational procedure. Nevertheless, the fact that the drop of mobility at this temperature is only slight gives confidence that the calculated values of mobilities around this temperature still represent a reasonable estimate of the true mobility in this range of temperatures. To further assess the abruptness of this apparent transition using the whole function rather than

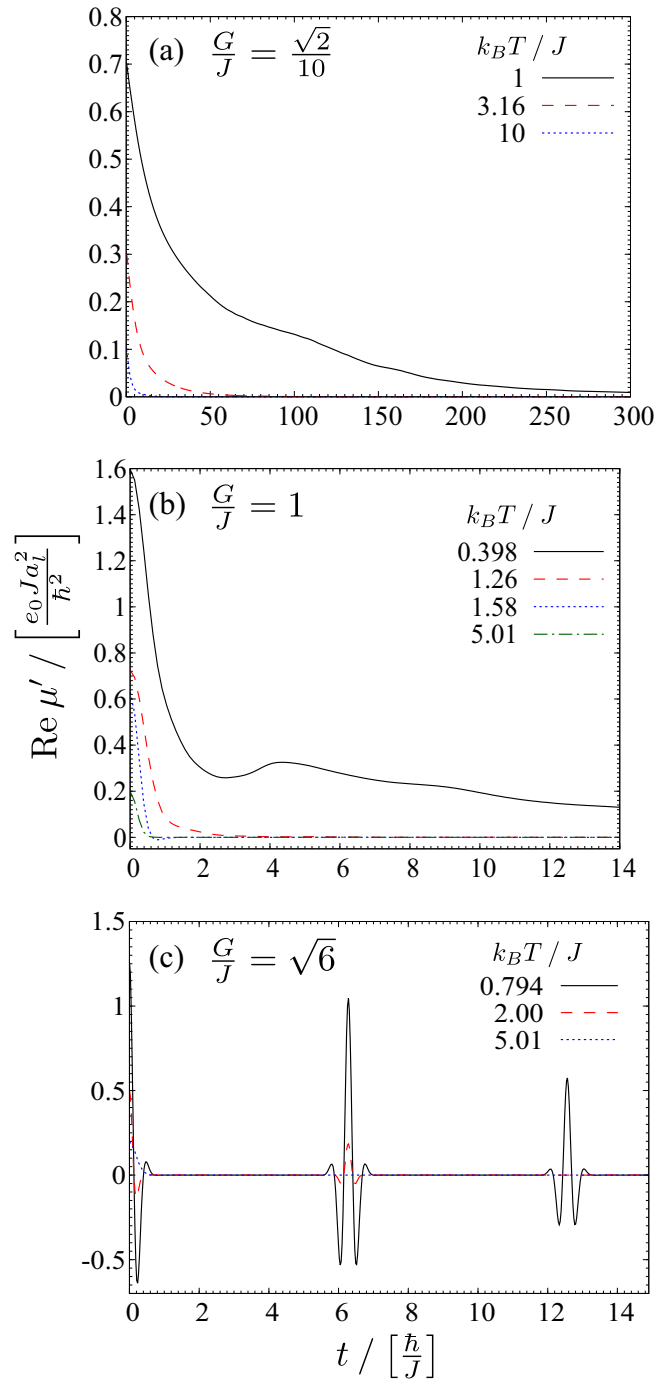


FIG. 6. Time dependence of the real part of the quantity $\mu'(t)$, which is proportional to current-current correlation function and whose integral over time is equal to mobility. The dependence is shown for $\frac{\hbar\Omega}{J} = 1$ and (a) $\frac{G}{J} = \frac{\sqrt{2}}{10}$, (b) $\frac{G}{J} = 1$, and (c) $\frac{G}{J} = \sqrt{6}$. Since the relation $\text{Re}\mu'(t) = \text{Re}\mu'(-t)$ holds, only the part with $t > 0$ is shown.

a single number, we present in Fig. 6(b) the real part of the quantity $\mu'(t)$ at temperatures before and after the transition in the case $\frac{G}{J} = 1$ and $\frac{\hbar\Omega}{J} = 1$. By comparing the dashed line at the temperature just before the transition and the dotted line at a temperature just after the transition, we see rather similar behavior of the $\mu'(t)$ dependence. This gives further confidence

that our estimate of mobility in this range of temperatures is reasonable. It is important to note that the discontinuity of the mobility is only slight (being much smaller than the discontinuity of the unitary transformation parameters) due to the fact that the transformed Hamiltonian was partitioned in such a way to minimize the effects of residual interaction and that the effects of interaction were then included up to lowest nontrivial order.

4. Large phonon energy

In the case of large phonon energy $\frac{\hbar\Omega}{J} = 3$, for interaction strengths $\frac{G}{J} \lesssim 4$ it is not possible to apply the formulas for the weak and strong electron-phonon coupling limits, derived in previous sections. Namely, in the case of low electron-phonon interaction and $\frac{\hbar\Omega}{J} > 2$, the perturbative formula given in Eq. (48) gives an infinite lifetime for \mathbf{k} points in the middle of the band for which neither absorption nor emission of phonons is allowed. This would then lead to infinite mobility. On the other hand, in the case of a strong electron-phonon interaction, we see from Fig. 3 that the spectral function keeps the momentum dependence and one cannot use the strong electron-phonon coupling derivation where it was assumed that this dependence was lost.

As in previous cases, the linewidth of the spectral function becomes narrow at small temperature. It is then numerically challenging to perform the calculation due to small linewidth of the spectral function, and at the same time none of the previously derived weak- or strong-coupling limits can be applied. To perform the calculation in the case of low temperature as well, we employ a different strategy. Our aim is to calculate the self-energy $\Sigma_{\mathbf{k}}(\omega)|_{\hbar\omega=e_{\mathbf{k}}-\mu_F}$ (which will further be denoted briefly as $\Sigma_{\mathbf{k}}$) at the frequency where the spectral function $A_{\mathbf{k}}(\omega - \mu_F)$ has a maximum for a given \mathbf{k} . The energy $e_{\mathbf{k}}$ is given as

$$e_{\mathbf{k}} = E_{\mathbf{k}} + \hbar \text{Re}\Sigma_{\mathbf{k}}. \quad (67)$$

We further use the fact that all contributions to self-energies are related to the Green's function by the relation of the form

$$\Sigma_{\mathbf{k}}^{(a)}(\omega) = \frac{1}{N_{\mathbf{k}}} \sum_{\mathbf{q}} \chi^{(a)}(\mathbf{k}, \mathbf{q}) G_{\mathbf{k}+\mathbf{q}}^R(\omega + n\Omega) \quad (68)$$

and we obtain the equation

$$\Sigma_{\mathbf{k}}^{(a)} = \frac{1}{N_{\mathbf{k}}} \sum_{\mathbf{q}} \frac{\chi^{(a)}(\mathbf{k}, \mathbf{q})}{\frac{e_{\mathbf{k}} - e_{\mathbf{k}+\mathbf{q}}}{\hbar} + n\Omega - i \cdot \text{Im}\Sigma_{\mathbf{k}+\mathbf{q}}}. \quad (69)$$

To find the $\Sigma_{\mathbf{k}}$ terms, we start with some initial guess. Then we use Eq. (69) to evaluate the contributions $\Sigma_{\mathbf{k}}^{(a)}$ which we add up to obtain the new $\Sigma_{\mathbf{k}}$. This procedure is repeated until convergence is reached. In Appendix E we provide the details of performing the summation in Eq. (69), which should be done carefully since the denominator may take rather small values.

To evaluate the mobility, we then assume spectral function in the form

$$A_{\mathbf{k}}(\omega - \mu_F) = \pi \alpha_{\mathbf{k}} e^{-\alpha_{\mathbf{k}} |\omega - \frac{e_{\mathbf{k}}}{\hbar}|}, \quad (70)$$

where $\alpha_{\mathbf{k}} = -\frac{2}{\pi \text{Im}\Sigma_{\mathbf{k}}}$. This choice of spectral function was made to satisfy the condition that it has the same maximum

as the spectral function $\frac{-2\text{Im}\Sigma_{\mathbf{k}}}{(\omega - \frac{c_{\mathbf{k}}}{\hbar})^2 + (\text{Im}\Sigma_{\mathbf{k}})^2}$ that would be obtained by assuming that $\Sigma_{\mathbf{k}}(\omega) = \Sigma_{\mathbf{k}}$, i.e., that the self-energy for a given \mathbf{k} does not depend on frequency. We have assumed the exponentially decaying shape of the spectral function in Eq. (70) since it was the best among several investigated shapes (Gaussian, Lorentzian, exponential). With the spectral function given by Eq. (70) at hand, we proceed to evaluate the mobility. The derivation of the corresponding expression is given in Appendix D.

The results presented in Fig. 4(c) indicate that the mobility decreases with an increase of temperature for electron-phonon interaction strengths $\frac{G}{J} \lesssim 4$. The dependencies are smooth as there is no temperature with a sharp change in parameters of the unitary transformation. The results obtained using the approach based on the narrow linewidth approximation [labeled as “nl” in Fig. 4(c)] are in excellent or reasonably good agreement with the results of the full calculation for lowest temperatures at which a full calculation could be performed. Some discrepancies originate from the assumptions used to calculate the mobility based on the narrow linewidth approximation. In particular, it was assumed that the spectral function has a single maximum, while we see in Fig. 3 some spectral weight redistribution, especially at high momenta. Nevertheless, the results obtained using the narrow linewidth approximation can be considered a very good estimate of the results at low temperatures.

5. Charge transport regimes

Next we discuss the charge carrier transport regimes for different system parameters. To facilitate the discussion, we estimated the mean free path of the charge carrier. It was estimated as

$$l_{\text{MFP}} = v_s \tau_c, \quad (71)$$

where v_s is the mean-square velocity of the carrier and τ_c is the coherence time. The coherence time was estimated from the decay of the correlation function $\mu'(t)$; when this decay is slower, coherence time is longer. The coherence time was quantified as

$$\tau_c = \frac{1}{2} \int_{-\infty}^{\infty} dt \left| \frac{\text{Re}\mu'(t)}{\text{Re}\mu'(0)} \right|. \quad (72)$$

The mean-square velocity was obtained from

$$v_s^2 = \frac{1}{N_c e_0^2} \langle j(0)j(0) \rangle. \quad (73)$$

The dependence of the mean free path on temperature for different system parameters is presented in Fig. 7. We generally find that the mean free path decreases as temperature increases.

At low electron-phonon interaction strength (for example, $\frac{G}{J} = \frac{\sqrt{2}}{10}$ for $\frac{\hbar\Omega}{J} = 1$) the mean free path is significantly larger than the lattice constant and conventional band transport takes place. The correlation function $\mu'(t)$ exhibits a slow decay, shown in Fig. 6(a). As the temperature increases, this decay becomes faster [see Fig. 6(a)] and the mean free path decreases but remains above the lattice constant. For somewhat larger interaction strengths (for example, $\frac{G}{J} = 1$ for $\frac{\hbar\Omega}{J} = 1$)

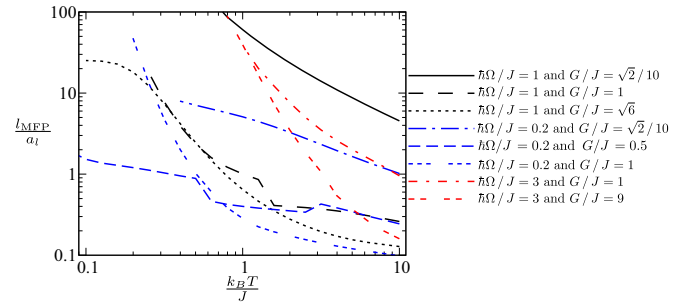


FIG. 7. Temperature dependence of the mean free path for different values of system parameters.

at a certain temperature the mean free path reaches the lattice constant (Mott-Ioffe-Regel limit) and the transport becomes incoherent, as can be also verified by fast decay of the correlation function in Fig. 6(b). Finally, for large interaction strength (for example, $\frac{G}{J} = \sqrt{6}$ for $\frac{\hbar\Omega}{J} = 1$) the mean free path at low temperature is significantly larger than the lattice constant, while the correlation function exhibits a series of peaks whose envelope slowly decays. In this regime, one can consider that the system consists of small polarons localized to lattice sites. These polarons form a narrow band due to electronic coupling between the sites. The transport can then be thought of as polaron-coherent band transport in such a narrow band. As the temperature increases, the mean free path reduces toward the lattice constant and the transport turns into a thermally activated small-polaron hopping. Further increase of temperature leads to small-polaron dissociation and turns the transport into an incoherent regime.

Overall, we find for all system parameters the crossover from coherent transport at low temperatures toward incoherent transport at high temperatures. The difference between the case with small and large electron-phonon interaction comes from the fact that small-polaron formation takes place at large electron-phonon interactions. For this reason a thermally activated region occurs when small-polaron dissociation takes place, while this region is absent for small electron-phonon interaction. Time dependence of the correlation function is an excellent signature of the transport regime. The high-temperature incoherent regime can be identified by a correlation function with a single pronounced peak at $t = 0$ which decays to zero on a timescale smaller than the phonon oscillation period [see, for example, the results in Figs. 6(b) and 6(c) for $\frac{k_B T}{J} > 1$]. On the other hand, coherent regimes can be identified by a correlation function that slowly decays over many phonon oscillation periods. In the case of small electron-phonon interaction strength it exhibits a continuous decay [see, for example, Fig. 6(a)], while in the case of large electron-phonon interactions it consists of a series of peaks whose amplitude decays slowly [see, for example, the full line in Fig. 6(c)].

While the discussion in this section was illustrated with example for the $\frac{\hbar\Omega}{J} = 1$ case, all comments remain valid also for other $\frac{\hbar\Omega}{J}$ ratios, as can be checked by analyzing the results presented in Figs. 1, 4, and 7. An interesting additional effect for $\frac{\hbar\Omega}{J} = 0.2$ and intermediate values of electron-phonon coupling (for example, $\frac{G}{J} = 0.5$) is the presence of region

with nonpolaronic charge carriers but with mean free path comparable to lattice spacing. Such regions are believed to be of interest for description of small-molecule-based organic semiconductors [48]. This region is present at temperatures in the range $\frac{k_B T}{J} \sim (0.1 - 0.5)$ for $\frac{G}{J} = 0.5$ (see Figs. 4 and 7).

IV. DISCUSSION AND CONCLUSION

Next we compare our approach to other related studies.

In Ref. [40] the authors also investigated the model with local electron-phonon coupling using the approach based on unitary transformation of the Hamiltonian and the use of Kubo's formula for mobility. There are two main differences between their work and our work: (i) In Ref. [40] Lang-Firsov transformation with fixed parameters was used, while we optimize the parameters of the transformation to minimize the effects of residual interacting part of the Hamiltonian. (ii) In Ref. [40] the mobility is evaluated by taking the averages with respect to diagonal part of the transformed Hamiltonian. Such an approach would lead to infinite mobility since time decay of current-current correlation function is not captured. This was overcome in Ref. [40] by introduction of coherence time τ through an additional $e^{-(\frac{\tau}{t})^2}$ factor in Kubo's formula, which was justified on physical grounds by the presence of interactions other than electron-phonon interaction in a real material. This parameter is, however, extrinsic to the initial model Hamiltonian. On the other hand, in our approach the time decay of current-current correlation function comes out naturally from finite width of the spectral function that leads to time decay of the $\langle a_{\mathbf{k}}(t)^\dagger a_{\mathbf{k}} \rangle$ and $\langle a_{\mathbf{k}}(t) a_{\mathbf{k}}^\dagger \rangle$ terms in Eq. (40).

In Ref. [38] the mobility within the Holstein model was also analyzed using a unitary transformation of the Hamiltonian, followed by calculation of mobility from quantum master equations for density matrices. We have fully followed Ref. [38] regarding the choice of unitary transformation and its parameters and there are no differences in that regard. On the other hand, the two approaches for mobility calculation are rather different. In particular, in Ref. [38] a finite phonon lifetime was introduced to avoid certain singularities, as well as additional scattering rate that mimics other interactions. As we already pointed out, our approach does not require introduction of such parameters extrinsic to initial model Hamiltonian.

Despite the fact that Holstein model is the most widely studied model of electron-phonon interaction, the mobility in the Holstein model was investigated using a fully many-body approach, such as quantum Monte Carlo, only recently [32]. The reason for this probably lies in the fact that calculation of finite-temperature correlation functions in quantum Monte Carlo is significantly more challenging than, for example, the calculation of ground-state energies. In the case $\frac{\hbar\Omega}{J} = 1$, the authors of Ref. [32] find that mobility decreases as the temperature increases when electron-phonon coupling is small, while the dependence exhibiting one minimum and one maximum is obtained for large electron-phonon coupling [see Fig. 3(a) in Ref. [32] and Fig. 8]. Exactly the same behavior is obtained in our calculations for $\frac{\hbar\Omega}{J} = 1$. This is rather satisfying given the fact that we restrict the calculation of self-energy to lowest nontrivial term in expansion in terms of

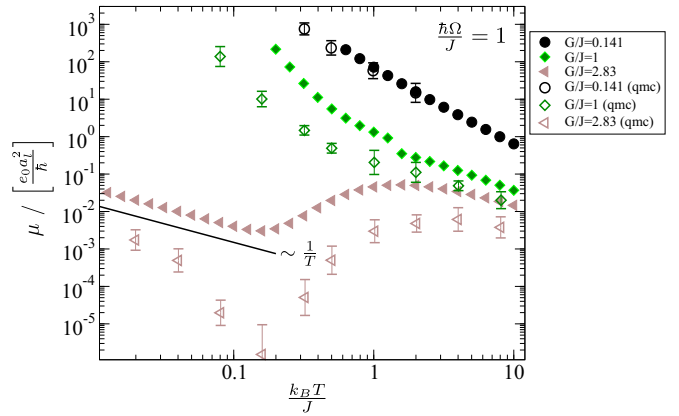


FIG. 8. Comparison of temperature dependence of mobility obtained in this work (unlabeled data sets) with quantum Monte Carlo results of Ref. [32] (data sets labeled as “qmc”). The straight line labeling the $\sim \frac{1}{T}$ dependence is given as a guide to the eye.

dressed Green's functions and that we restrict the evaluation of mobility also to lowest nontrivial term. On the other hand, a fully quantitative agreement of our results with quantum Monte Carlo results of Ref. [32] could not be achieved. This comparison is presented in Fig. 8. The agreement is excellent at low electron-phonon coupling strengths. At intermediate electron-phonon coupling our results are somewhat above the range of Monte Carlo statistical error interval for high temperatures and deviate more at lower temperatures, while for large electron-phonon coupling our results are systematically above the quantum Monte Carlo results. It would be certainly of strong interest for future studies to understand the origin of these differences and to improve the quantitative agreement between the two approaches. At present, we comment on the results at lowest temperatures and largest electron-phonon coupling strengths [say, $\frac{k_B T}{J} \in (0.01 - 0.1)$ and $\frac{G}{J} = 2.83$]. In this parameter range the lowest eigenstates of \tilde{H} form a narrow band spanned by the states $a_{\mathbf{k}}^\dagger |\text{vac}\rangle$, where $|\text{vac}\rangle$ is the vacuum state. The dispersion of this band has the width of approximately $W_b = 4J e^{-(\frac{G}{\hbar\Omega})^2}$. The next band formed by the states $a_{\mathbf{k}}^\dagger b_{\mathbf{R}}^\dagger |\text{vac}\rangle$ is approximately at energy $\hbar\Omega$ above the lowest band. Exact result for the mobility reads [43]
$$\mu = \frac{\pi \beta \sum_{n,m} e^{-\beta \tilde{E}_n} |\langle m | \tilde{j} | n \rangle|^2 \delta(\tilde{E}_m - \tilde{E}_n)}{\sum_m e^{-\beta \tilde{E}_m}},$$
 where $|m\rangle$ and \tilde{E}_n denote the eigenvectors and eigenvalues of \tilde{H} . In this parameter range the following inequalities hold: $k_B T \gg W_b$ and $k_B T \ll \hbar\Omega$. Therefore, only the lowest band contributes to the mobility and the term $e^{-\beta \tilde{E}_n}$ is approximately 1 (if the energies are measured with respect to the bottom of the lowest band). Consequently, the $\sim \frac{1}{T}$ dependence of mobility on temperature is expected since only the β prefactor in the expression for μ introduces the temperature dependence. Such a dependence is indeed obtained in our approach (see Fig. 8) but not in quantum Monte Carlo results of Ref. [32].

There is also a variety of studies where electrical transport in system of electrons that interact with lattice is modeled using a mixed quantum-classical approach [48–52]. In these approaches electrons are treated as quantum particles, while the lattice is treated classically. One of the issues with such an approach is that summations with Ehrenfest dynamics lead

to overheating of the electronic subsystem [53]. This issue can be overcome to a large extent using a surface-hopping approach [54] and its modifications and extensions [50,51]. Nevertheless, classical approximation for lattice motion can be valid only at sufficiently high temperatures, while at low temperatures quantum description of lattice motion is inevitable. In Ref. [55] the mobility was evaluated using Kubo's formula, where integral of current-current correlation function was evaluated using analytic continuation and the saddle-point approximation. It remains unclear whether the approximations of the method will be valid throughout the whole range of relevant system parameters.

There is a variety of works on organic semiconductors where mobility is calculated by assuming carrier hopping from one site to another with hopping rates determined as [56,57]

$$W = \frac{J^2}{\hbar^2} \int_{-\infty}^{\infty} dt e^{-2\sum_f \left(\frac{G_f}{\hbar\Omega_f}\right)^2 [(n_f^{\text{ph}}+1)e^{-i\Omega_f t} + n_f^{\text{ph}} e^{i\Omega_f t}]} \quad (74)$$

or using the Marcus formula [58–62]

$$W = \frac{J^2}{\hbar} \sqrt{\frac{\pi}{k_B T \Lambda}} e^{-\frac{\Lambda}{4k_B T}} \quad (75)$$

with $\Lambda = 2\sum_f \frac{G_f^2}{\hbar\Omega_f}$. The mobility can then be obtained from the Einstein relation between the diffusion coefficient and mobility, which, in the case of one dimension, leads to

$$\mu = \frac{e_0 a_l^2}{k_B T} W. \quad (76)$$

The mobility given by Eqs. (74) and (76) can be obtained from Eq. (56) by assuming that the spectral function takes the form of a delta function, in which case the $\langle a(t)^\dagger a \rangle \langle a(t) a^\dagger \rangle$ term in Eq. (56) becomes a constant. The mobility obtained from Eqs. (75) and (76) can be obtained by introducing several further approximations, such as (i) a short-time approximation of exponential terms $e^{\pm i\Omega_f t} = 1 \pm i\Omega_f t - \frac{1}{2}\Omega_f^2 t^2$ and (ii) a high-temperature approximation $2n_f^{\text{ph}} + 1 = \frac{2k_B T}{\hbar\Omega_f}$ which is valid for $k_B T \gg \hbar\Omega_f$. We further note that the integral given in Eq. (74) is divergent in the case of single-phonon mode, since the function under the integral is periodic with period $\frac{2\pi}{\Omega}$ (note that in realistic systems phonon-phonon interaction and other carrier scattering mechanism lead to decay of the function in the integral in Eq. (74) and the absence of this divergence). In the case of multiple-phonon modes, the period (if it exists) is determined from the lowest common multiple of periods $\frac{2\pi}{\Omega_f}$. In practice, for large electron-phonon couplings in the case of multiple-phonon modes, the function under the integral in Eq. (74) quickly decays to zero and the integral can be straightforwardly numerically calculated [56,63]. This discussion points out to the limits of mobility expressions Eqs. (74)–(76) and Eqs. (75) and (76). Equations (74)–(76) are valid for strong electron-phonon coupling and narrow linewidth of the spectral function, while additional condition for the validity of (75) and (76) is high temperature. The results presented in Fig. 4 suggest that Eqs. (75) and (76) give most reliable results for smallest $\frac{\hbar\Omega}{J}$ at high temperatures.

Next, we discuss the possibility of using the main ideas of our approach for other electron-phonon interaction Hamil-

tonians. In this work, we have focused on Hamiltonians with local electron-phonon interaction, where phonon mode at a certain site couples with an electron from the same site as described by the $a_{\mathbf{R}}^\dagger a_{\mathbf{R}} (b_{\mathbf{R}} + b_{\mathbf{R}}^\dagger)$ term. In this case, unitary transformation that we use leads to exact diagonalization of the Hamiltonian in the limits of strong and weak electron-phonon interaction. For this reason, it is expected that for other cases, the remaining nondiagonal part of the transformed Hamiltonian can be treated perturbatively. In a recent work, the same unitary transformation was successfully applied to a one-dimensional lattice version of the Fröhlich Hamiltonian where phonon mode couples also to electrons from other sites [64], as described by the $a_{\mathbf{R}}^\dagger a_{\mathbf{R}} (b_{\mathbf{S}} + b_{\mathbf{S}}^\dagger)$ term. The most general form of the Hamiltonian includes also the terms where the phonon from a certain site modifies the electronic transfer integral between other sites, as described by the $a_{\mathbf{R}}^\dagger a_{\mathbf{S}} (b_{\mathbf{T}} + b_{\mathbf{T}}^\dagger)$ terms. On the technical side, there are no obstacles in applying the same unitary transformation in this case as well. However, it is questionable whether the remaining nondiagonal term will be small then. Nevertheless, one can then apply a more general unitary transformation, where nonlocal terms would be included in the transformation [65–67]. The results of these calculations could then be compared to available quantum Monte Carlo results [68].

In conclusion, we presented an approach for calculation of finite-temperature mobility in systems with local electron-phonon interaction. The approach combines unitary transformation of the Hamiltonian, Matsubara Green's function technique for evaluation of spectral functions, and Kubo's linear response theory for calculation of mobility. It was demonstrated that the approach yields physically plausible results for temperature dependence of mobility in the Holstein model, without introducing any regularization parameters extrinsic to the model Hamiltonian. It is expected that with appropriate modifications of the unitary transformation the approach could be also applicable to more general Hamiltonians. Bearing in mind that the approach is computationally relatively inexpensive, it holds promise for future applications to electron-phonon interaction Hamiltonians obtained from *ab initio* calculations of realistic materials.

ACKNOWLEDGMENTS

We gratefully acknowledge the support by the Ministry of Education, Science and Technological Development of the Republic of Serbia (Project No. ON171017) and the European Commission under H2020 project VI-SEEM, Grant No. 675121, and contribution of the COST Action MP1406. Numerical computations were performed on the PARADOX supercomputing facility at the Scientific Computing Laboratory of the Institute of Physics Belgrade.

APPENDIX A: UPPER BOUND ON FREE ENERGY AND EQUATION FOR OPTIMAL PARAMETERS OF UNITARY TRANSFORMATION IN THE ONE-DIMENSIONAL CASE

In this section, we present explicit formulas for upper bound on free energy and for optimal parameters of unitary transformation in the case of a one-dimensional model

with nearest-neighbor electronic coupling J . In this case, the energy dispersion $E_{\mathbf{k}}$ reduces to

$$E_{\mathbf{k}} = E' - 2J_{\text{eff}} \cos(ka_l), \quad (\text{A1})$$

where

$$J_{\text{eff}} = J\theta_{a_l}^{(0)}. \quad (\text{A2})$$

The upper bound on free energy is given as

$$F_{ub} = -k_B T \ln \sum_{\mathbf{k}} e^{-\beta E_{\mathbf{k}}}. \quad (\text{A3})$$

After replacement of the sum $\sum_{\mathbf{k}}$ with corresponding integral $\frac{N_k a_l}{2\pi} \int_{-\pi/a_l}^{\pi/a_l} dk$ and using the identity $I_0(z) = \frac{1}{\pi} \int_0^\pi e^{z \cos \theta} d\theta$, we come to the expression

$$F_{ub} = E' - k_B T \ln I_0(2\beta J_{\text{eff}}). \quad (\text{A4})$$

We search for the parameters $D_{n,f}$ that minimize F_{ub} . By setting partial derivatives $\frac{\partial F_{ub}}{\partial D_{n,f}}$ to zero, we obtain the expression

$$\begin{aligned} D_{n,f} + \frac{J_{\text{eff}}}{\hbar \Omega_f} \frac{I_1(2\beta J_{\text{eff}})}{I_0(2\beta J_{\text{eff}})} (2n_f^{\text{ph}} + 1) (2D_{n,f} - D_{n-1,f} - D_{n+1,f}) \\ = \frac{G_f}{\hbar \Omega_f} \delta_{n,0}. \end{aligned} \quad (\text{A5})$$

Equation (A2) can be rewritten in the form

$$J_{\text{eff}} = J e^{-\sum_{n,f} (D_{n,f} - D_{n-1,f})^2 (n_f^{\text{ph}} + \frac{1}{2})}. \quad (\text{A6})$$

We use Eqs. (A5) and (A6) to find the parameters $D_{n,f}$. In more detail, for given J_{eff} the expression (A5) can be considered as a system of linear equations for unknown parameters $D_{n,f}$. By replacing the solution of this system in Eq. (A6), this equation becomes a nonlinear equation with a single unknown variable J_{eff} . We find all its solutions using the bisection method. When the number of solutions is larger than 1, we choose the solution with smallest F_{ub} .

APPENDIX B: EVALUATION OF SELF-ENERGIES AND SPECTRAL FUNCTIONS

The Matsubara Green's function is defined as

$$\mathcal{G}_{\mathbf{k}}(\tau) = -\langle T_\tau a_{\mathbf{k}}^{\tilde{H}}(\tau) a_{\mathbf{k}}^{\dagger} \rangle_{\tilde{H}}, \quad (\text{B1})$$

where

$$a_{\mathbf{k}}^{\tilde{H}}(\tau) = e^{\frac{\tau}{\hbar}(\tilde{H} - \mu_F N)} a_{\mathbf{k}} e^{-\frac{\tau}{\hbar}(\tilde{H} - \mu_F N)} \quad (\text{B2})$$

and averaging $\langle \dots \rangle_{\tilde{H}}$ denotes the grand-canonical ensemble average

$$\langle X \rangle_{\tilde{H}} = \frac{\text{Tr}[X e^{-\beta(\tilde{H} - \mu_F N)}]}{\text{Tr}[e^{-\beta(\tilde{H} - \mu_F N)}]}, \quad (\text{B3})$$

while T_τ denotes the τ -ordering operator, which arranges operators with earliest τ to the right. $\mathcal{G}_{\mathbf{k}}(\tau)$ can further be expressed as

$$\mathcal{G}_{\mathbf{k}}(\tau) = -\frac{\langle T_\tau S(\hbar\beta) a_{\mathbf{k}}^{\tilde{H}_0}(\tau) a_{\mathbf{k}}^{\dagger} \rangle_{\tilde{H}_0}}{\langle S(\hbar\beta) \rangle_{\tilde{H}_0}}. \quad (\text{B4})$$

The operator $S(\hbar\beta)$ is given via Dyson's series as

$$\begin{aligned} S(\hbar\beta) = \sum_{n=0}^{\infty} \frac{(-1)^n}{n! \cdot \hbar^n} \int_0^{\hbar\beta} d\tau_1 \dots \\ \times \int_0^{\hbar\beta} d\tau_n T_\tau [\tilde{V}^{\tilde{H}_0}(\tau_1) \dots \tilde{V}^{\tilde{H}_0}(\tau_n)]. \end{aligned} \quad (\text{B5})$$

To evaluate the Matsubara Green's function given in Eq. (B4) we restrict ourselves up to terms quadratic in the interaction \tilde{V} which is the lowest order that gives a nontrivial contribution. We consider only the connected diagrams from the nominator because the contribution of disconnected diagrams cancels exactly the diagrams in the denominator. The Green's function then reads

$$\begin{aligned} \mathcal{G}_{\mathbf{k}}(\tau) = \mathcal{G}_{\mathbf{k}}^{(0)}(\tau) - \frac{1}{2N_k^2 \hbar^2} \int_0^{\hbar\beta} d\tau_1 \int_0^{\hbar\beta} d\tau_2 \sum_{\mathbf{k}_1, \mathbf{q}_1, \mathbf{k}_2, \mathbf{q}_2} \langle T_\tau \mathcal{B}_{\mathbf{k}_1, \mathbf{q}_1}^{\tilde{H}_0}(\tau_1) \mathcal{B}_{\mathbf{k}_2, \mathbf{q}_2}^{\tilde{H}_0}(\tau_2) \rangle_{\tilde{H}_0} \\ \times \langle T_\tau a_{\mathbf{k}}^{\tilde{H}_0}(\tau) a_{\mathbf{k}_1 + \mathbf{q}_1}^{\tilde{H}_0}(\tau_1)^\dagger a_{\mathbf{k}_1}^{\tilde{H}_0}(\tau_1) a_{\mathbf{k}_2 + \mathbf{q}_2}^{\tilde{H}_0}(\tau_2)^\dagger a_{\mathbf{k}_2}^{\tilde{H}_0}(\tau_2) a_{\mathbf{k}}^{\dagger} \rangle_{\tilde{H}_0}, \end{aligned} \quad (\text{B6})$$

where $\mathcal{G}_{\mathbf{k}}^{(0)}(\tau)$ is the Matsubara Green's function for the noninteracting Hamiltonian. Using Wick's theorem we obtain

$$\begin{aligned} \langle T_\tau a_{\mathbf{k}}^{\tilde{H}_0}(\tau) a_{\mathbf{k}_1 + \mathbf{q}_1}^{\tilde{H}_0}(\tau_1)^\dagger a_{\mathbf{k}_1}^{\tilde{H}_0}(\tau_1) a_{\mathbf{k}_2 + \mathbf{q}_2}^{\tilde{H}_0}(\tau_2)^\dagger a_{\mathbf{k}_2}^{\tilde{H}_0}(\tau_2) a_{\mathbf{k}}^{\dagger} \rangle_{\tilde{H}_0} \\ = -\delta_{\mathbf{k}, \mathbf{k}_1 + \mathbf{q}_1} \delta_{\mathbf{k}_1, \mathbf{k}_2 + \mathbf{q}_2} \delta_{\mathbf{k}, \mathbf{k}_2} \mathcal{G}_{\mathbf{k}}^{(0)}(\tau - \tau_1) \mathcal{G}_{\mathbf{k}_1}^{(0)}(\tau_1 - \tau_2) \mathcal{G}_{\mathbf{k}_2}^{(0)}(\tau_2) \\ - \delta_{\mathbf{k}, \mathbf{k}_2 + \mathbf{q}_2} \delta_{\mathbf{k}_2, \mathbf{k}_1 + \mathbf{q}_1} \delta_{\mathbf{k}, \mathbf{k}_1} \mathcal{G}_{\mathbf{k}}^{(0)}(\tau - \tau_2) \mathcal{G}_{\mathbf{k}_2}^{(0)}(\tau_2 - \tau_1) \mathcal{G}_{\mathbf{k}_1}^{(0)}(\tau_1). \end{aligned} \quad (\text{B7})$$

In the last expression the terms that would lead to disconnected diagrams were excluded. The terms that contain the factors proportional to the number of carriers were also excluded since these vanish in the limit of low carrier concentration. The term with phonon operators reads

$$-\langle T_\tau \mathcal{B}_{\mathbf{k}_1, \mathbf{q}_1}^{\tilde{H}_0}(\tau_1) \mathcal{B}_{\mathbf{k}_2, \mathbf{q}_2}^{\tilde{H}_0}(\tau_2) \rangle_{\tilde{H}_0} = N_k \delta_{\mathbf{q}_1, -\mathbf{q}_2} \mathcal{D}_{\mathbf{k}_1, \mathbf{k}_2, \mathbf{q}_1}(\tau_1 - \tau_2), \quad (\text{B8})$$

where

$$\begin{aligned} \mathcal{D}_{\mathbf{k}_1, \mathbf{k}_2, \mathbf{q}_1}(\tau_1 - \tau_2) = & - \sum_f \phi_{\mathbf{q}_1, f}^2 [n_f^{\text{ph}} e^{\Omega_f |\tau_1 - \tau_2|} + (n_f^{\text{ph}} + 1) e^{-\Omega_f |\tau_1 - \tau_2|}] \\ & - \sum_{\mathbf{X}, \mathbf{Y}, \mathbf{Z}} J_{\mathbf{X}} J_{\mathbf{Y}} e^{i\mathbf{k}_1 \cdot \mathbf{X}} e^{i\mathbf{k}_2 \cdot \mathbf{Y}} e^{i\mathbf{q}_1 \cdot \mathbf{Z}} \theta_{\mathbf{X}}^{(0)} \theta_{\mathbf{Y}}^{(0)} [\theta_{\mathbf{X}, \mathbf{Y}, \mathbf{Z}}(|\tau_1 - \tau_2|) - 1] \\ & + \sum_{\mathbf{X}, \mathbf{Z}, f} \phi_{\mathbf{q}_1, f} J_{\mathbf{X}} \theta_{\mathbf{X}}^{(0)} e^{i\mathbf{q}_1 \cdot \mathbf{Z}} (e^{i\mathbf{k}_2 \cdot \mathbf{X}} - e^{-i\mathbf{k}_1 \cdot \mathbf{X}}) (D_{\mathbf{Z}, f} - D_{\mathbf{Z} + \mathbf{X}, f}) \\ & \times [(n_f^{\text{ph}} + 1) e^{-\Omega_f |\tau_1 - \tau_2|} - n_f^{\text{ph}} e^{\Omega_f |\tau_1 - \tau_2|}] \text{sgn}(\tau_1 - \tau_2) \end{aligned} \quad (\text{B9})$$

and

$$\theta_{\mathbf{X}, \mathbf{Y}, \mathbf{Z}}(\tau) = \exp \left\{ - \sum_f \left[(n_f^{\text{ph}} + 1) e^{-\Omega_f \tau} + n_f^{\text{ph}} e^{\Omega_f \tau} \right] \sum_{\mathbf{U}} (D_{\mathbf{U}, f} - D_{\mathbf{U} + \mathbf{X}, f}) (D_{\mathbf{U} + \mathbf{Z}, f} - D_{\mathbf{U} + \mathbf{Z} + \mathbf{Y}, f}) \right\}. \quad (\text{B10})$$

Using Eqs. (B6)–(B8) we find

$$\mathcal{G}_{\mathbf{k}}(\tau) = \mathcal{G}_{\mathbf{k}}^{(0)}(\tau) + \int_0^{\hbar\beta} d\tau_1 \int_0^{\hbar\beta} d\tau_2 \mathcal{G}_{\mathbf{k}}^{(0)}(\tau - \tau_1) \left[\frac{-1}{N_k \hbar^2} \sum_{\mathbf{q}} \mathcal{D}_{\mathbf{k}-\mathbf{q}, \mathbf{k}, \mathbf{q}}(\tau_1 - \tau_2) \mathcal{G}_{\mathbf{k}-\mathbf{q}}^{(0)}(\tau_1 - \tau_2) \right] \mathcal{G}_{\mathbf{k}}^{(0)}(\tau_2). \quad (\text{B11})$$

In the last expression one can directly read the self-energy as

$$\Sigma_{\mathbf{k}}(\tau) = \frac{-1}{N_k \hbar^2} \sum_{\mathbf{q}} \mathcal{D}_{\mathbf{k}-\mathbf{q}, \mathbf{k}, \mathbf{q}}(\tau) \mathcal{G}_{\mathbf{k}-\mathbf{q}}^{(0)}(\tau). \quad (\text{B12})$$

Next, we transform the last expression to the Matsubara frequency domain by using the relations between the Green's functions or self-energies in the time and frequency domain that read:

$$\mathcal{G}(\tau) = \frac{1}{\hbar\beta} \sum_n e^{-i\omega_n \tau} \mathcal{G}(i\omega_n), \quad (\text{B13})$$

$$\mathcal{G}(i\omega_n) = \int_0^{\hbar\beta} d\tau \mathcal{G}(\tau) e^{i\omega_n \tau}, \quad (\text{B14})$$

where $\omega_n = \frac{(2n+1)\pi}{\hbar\beta}$ for fermionic Green's function and self-energies, while $\omega_n = \frac{2n\pi}{\hbar\beta}$ for bosonic Green's function and self-energies. We come to the expression

$$\Sigma_{\mathbf{k}}(i\omega_n) = \frac{-1}{N_k \hbar^2} \sum_{\mathbf{q}} \frac{1}{\hbar\beta} \sum_m \mathcal{D}_{\mathbf{k}-\mathbf{q}, \mathbf{k}, \mathbf{q}}(i\omega_n - i\omega_m) \mathcal{G}_{\mathbf{k}-\mathbf{q}}^{(0)}(i\omega_m). \quad (\text{B15})$$

Next, we evaluate retarded self-energy by performing analytic continuation of Eq. (B15). To this end, we first express $\mathcal{D}_{\mathbf{k}-\mathbf{q}, \mathbf{k}, \mathbf{q}}(i\omega_n - i\omega_m)$ and $\mathcal{G}_{\mathbf{k}-\mathbf{q}}^{(0)}(i\omega_m)$ in terms of correspondent spectral functions $D_{\mathbf{k}-\mathbf{q}, \mathbf{k}, \mathbf{q}}(\omega)$ and $A_{\mathbf{k}-\mathbf{q}}^{(0)}(\omega)$ as

$$D_{\mathbf{k}-\mathbf{q}, \mathbf{k}, \mathbf{q}}(i\omega_n - i\omega_m) = \frac{1}{2\pi} \int_{-\infty}^{\infty} d\omega_1 \frac{D_{\mathbf{k}-\mathbf{q}, \mathbf{k}, \mathbf{q}}(\omega_1)}{i\omega_n - i\omega_m - \omega_1}, \quad (\text{B16})$$

$$\mathcal{G}_{\mathbf{k}-\mathbf{q}}^{(0)}(i\omega_m) = \frac{1}{2\pi} \int_{-\infty}^{\infty} d\omega_2 \frac{A_{\mathbf{k}-\mathbf{q}}^{(0)}(\omega_2)}{i\omega_m - \omega_2}. \quad (\text{B17})$$

To evaluate the sum $\sum_m \frac{1}{\hbar\beta} \frac{1}{i\omega_n - i\omega_m - \omega_1} \frac{1}{i\omega_m - \omega_2}$, we define an auxiliary function h of complex variable z as

$$h(z) = -n_F(z) \frac{1}{z - (i\omega_n - \omega_1)} \frac{1}{z - \omega_2}, \quad (\text{B18})$$

where $n_F(z) = \frac{1}{e^{\hbar\beta z} + 1}$ is the Fermi-Dirac function. The function $h(z)$ decays faster than $\frac{1}{|z|}$ as $|z| \rightarrow \infty$ and, consequently,

$$\oint_C h(z) dz = 0, \quad (\text{B19})$$

where contour C is a circle with an infinitely large radius. On the other hand, the same integral can be calculated using Cauchy's residue theorem. Poles of the function $h(z)$ are at $i\omega_m$, $i\omega_n - \omega_1$, and ω_2 and, consequently,

$$\oint_C h(z) dz = 2\pi i \left[\frac{1}{\beta\hbar} \sum_m \frac{1}{i\omega_m - i\omega_n + \omega_1} \frac{1}{i\omega_m - \omega_2} - \frac{n_F(i\omega_n - \omega_1)}{i\omega_n - \omega_1 - \omega_2} - \frac{n_F(\omega_2)}{\omega_2 - i\omega_n + \omega_1} \right]. \quad (\text{B20})$$

Using the identity $n_F(i\omega_n - \omega_1) = -n_B(-\omega_1)$ [where $n_B(z) = \frac{1}{e^{\hbar\beta z} - 1}$ is the Bose-Einstein function], neglecting the $n_F(\omega_2)$ term which vanishes in the limit of low carrier concentration, Eqs. (B19) and (B20) lead to

$$\sum_m \frac{1}{\hbar\beta} \frac{1}{i\omega_n - i\omega_m - \omega_1} \frac{1}{i\omega_m - \omega_2} = -\frac{n_B(-\omega_1)}{i\omega_n - \omega_1 - \omega_2}. \quad (\text{B21})$$

From Eqs. (B15)–(B17), and (B21) one obtains

$$\begin{aligned} \Sigma_{\mathbf{k}}(i\omega_n) = & \frac{1}{N_k \hbar^2} \frac{1}{(2\pi)^2} \sum_{\mathbf{q}} \int d\omega_1 d\omega_2 D_{\mathbf{k}-\mathbf{q}, \mathbf{k}, \mathbf{q}}(\omega_1) A_{\mathbf{k}-\mathbf{q}}^{(0)}(\omega_2) \\ & \times \frac{n_B(-\omega_1)}{i\omega_n - \omega_1 - \omega_2}. \end{aligned} \quad (\text{B22})$$

After performing analytic continuation by the substitution $i\omega_n \rightarrow \omega + i0^+$ and using the identity that relates the retarded Green's function $G_{\mathbf{k}-\mathbf{q}}^{(0),R}$ with the spectral function

$$G_{\mathbf{k}-\mathbf{q}}^{(0),R}(\omega - \omega_1) = \frac{1}{2\pi} \int d\omega_2 A_{\mathbf{k}-\mathbf{q}}^{(0)}(\omega_2) \frac{1}{\omega + i0^+ - \omega_1 - \omega_2} \quad (\text{B23})$$

and the identity that relates bosonic spectral function $D_{\mathbf{k}-\mathbf{q},\mathbf{k},\mathbf{q}}$ and greater function $D_{\mathbf{k}-\mathbf{q},\mathbf{k},\mathbf{q}}^>$

$$i n_B(-\omega_1) D_{\mathbf{k}-\mathbf{q},\mathbf{k},\mathbf{q}}(\omega_1) = D_{\mathbf{k}-\mathbf{q},\mathbf{k},\mathbf{q}}^>(\omega_1) \quad (\text{B24})$$

we obtain the expression for retarded self-energy

$$\Sigma_{\mathbf{k}}^R(\omega) = \frac{i}{2\pi N_k \hbar^2} \sum_{\mathbf{q}} \int d\omega_1 D_{\mathbf{k}-\mathbf{q},\mathbf{k},\mathbf{q}}^>(\omega_1) G_{\mathbf{k}-\mathbf{q}}^{(0),R}(\omega - \omega_1). \quad (\text{B25})$$

The greater function $D_{\mathbf{k}-\mathbf{q},\mathbf{k},\mathbf{q}}^>$ can be evaluated from its definition in the time domain

$$-i \langle \mathcal{B}_{\mathbf{k}_1, \mathbf{q}_1}(t) \mathcal{B}_{\mathbf{k}_2, \mathbf{q}_2}(0) \rangle_{\tilde{H}_0} = N_k \delta_{\mathbf{q}_1, -\mathbf{q}_2} D_{\mathbf{k}_1, \mathbf{k}_2, \mathbf{q}_1}^>(t). \quad (\text{B26})$$

After evaluation of the expectation value on the left-hand side of Eq. (B26), we obtain

$$\begin{aligned} D_{\mathbf{k}-\mathbf{q},\mathbf{k},\mathbf{q}}^>(\omega) &= -2\pi i \sum_f |\phi_{\mathbf{q},f}|^2 [n_f^{\text{ph}} \delta(\omega + \Omega_f) + (n_f^{\text{ph}} + 1) \delta(\omega - \Omega_f)] + 2\pi i \sum_{\mathbf{X}, \mathbf{Y}, f} \phi_{\mathbf{q}} J_{\mathbf{X}} (e^{i\mathbf{k} \cdot \mathbf{X}} - e^{-i(\mathbf{k}-\mathbf{q}) \cdot \mathbf{X}}) \\ &\quad \times e^{i\mathbf{q} \cdot \mathbf{Y}} \theta_{\mathbf{X}}^{(0)}(D_{\mathbf{Y},f} - D_{\mathbf{X}+\mathbf{Y},f}) [(n_f^{\text{ph}} + 1) \delta(\omega - \Omega_f) - n_f^{\text{ph}} \delta(\omega + \Omega_f)] \\ &\quad - i \sum_{\mathbf{X}, \mathbf{Y}, \mathbf{Z}} J_{\mathbf{X}} J_{\mathbf{Y}} \theta_{\mathbf{X}}^{(0)} \theta_{\mathbf{Y}}^{(0)} e^{i(\mathbf{k}-\mathbf{q}) \cdot \mathbf{X}} e^{i\mathbf{k} \cdot \mathbf{Y}} e^{i\mathbf{q} \cdot \mathbf{Z}} \int_{-\infty}^{\infty} dt e^{i\omega t} [\theta_{\mathbf{X}, \mathbf{Y}, \mathbf{Z}}(t) - 1]. \end{aligned} \quad (\text{B27})$$

From Eqs. (B25) and (B27) we obtain the final expression for retarded self-energy,

$$\Sigma_{\mathbf{k}}^R(\omega) = \Sigma_{\mathbf{k}}^{(1)}(\omega) + \Sigma_{\mathbf{k}}^{(2)}(\omega) + \Sigma_{\mathbf{k}}^{(3)}(\omega), \quad (\text{B28})$$

where

$$\Sigma_{\mathbf{k}}^{(1)}(\omega) = \frac{1}{N_k \hbar^2} \sum_{\mathbf{q}, f} |\phi_{\mathbf{q},f}|^2 [(n_f^{\text{ph}} + 1) G_{\mathbf{k}-\mathbf{q}}^{(0),R}(\omega - \Omega_f) + n_f^{\text{ph}} G_{\mathbf{k}-\mathbf{q}}^{(0),R}(\omega + \Omega_f)], \quad (\text{B29})$$

$$\begin{aligned} \Sigma_{\mathbf{k}}^{(2)}(\omega) &= \frac{-1}{N_k \hbar^2} \sum_{\mathbf{q}, f} \phi_{\mathbf{q},f} [(n_f^{\text{ph}} + 1) G_{\mathbf{k}-\mathbf{q}}^{(0),R}(\omega - \Omega_f) - n_f^{\text{ph}} G_{\mathbf{k}-\mathbf{q}}^{(0),R}(\omega + \Omega_f)] \\ &\quad \times \sum_{\mathbf{X}, \mathbf{Y}} J_{\mathbf{X}} \theta_{\mathbf{X}}^{(0)}(D_{\mathbf{Y},f} - D_{\mathbf{X}+\mathbf{Y},f}) e^{i\mathbf{q} \cdot \mathbf{Y}} [e^{i\mathbf{k} \cdot \mathbf{X}} - e^{-i(\mathbf{k}-\mathbf{q}) \cdot \mathbf{X}}], \end{aligned} \quad (\text{B30})$$

$$\Sigma_{\mathbf{k}}^{(3)}(\omega) = \frac{1}{N_k \hbar^2} \sum_{\mathbf{q}} \sum_{\mathbf{X}, \mathbf{Y}, \mathbf{Z}} J_{\mathbf{X}} J_{\mathbf{Y}} \theta_{\mathbf{X}}^{(0)} \theta_{\mathbf{Y}}^{(0)} e^{i(\mathbf{k}-\mathbf{q}) \cdot \mathbf{X}} e^{i\mathbf{k} \cdot \mathbf{Y}} e^{i\mathbf{q} \cdot \mathbf{Z}} \int_{-\infty}^{\infty} dt e^{i\omega t} [\theta_{\mathbf{X}, \mathbf{Y}, \mathbf{Z}}(t) - 1] G_{\mathbf{k}-\mathbf{q}}^{(0),R}(t). \quad (\text{B31})$$

APPENDIX C: MOBILITY IN THE LIMIT OF WEAK ELECTRON-PHONON COUPLING FOR THE HOLSTEIN MODEL

In this section, we derive the formula that is used to calculate the mobility in the limit of weak electron-phonon coupling for Holstein model with single-phonon mode. The scattering time is given as

$$\frac{1}{\tau_{\mathbf{k}}} = \frac{2\pi}{\hbar} \frac{1}{N_k} \sum_{\mathbf{q}} G^2 [(n^{\text{ph}} + 1) \delta(E_{\mathbf{k}} - \hbar\Omega - E_{\mathbf{k}-\mathbf{q}}) + n^{\text{ph}} \delta(E_{\mathbf{k}} + \hbar\Omega - E_{\mathbf{k}-\mathbf{q}})], \quad (\text{C1})$$

where $E_{\mathbf{k}} = -2J \cos(ka_l)$. After replacing the summation with corresponding integration, we obtain

$$\frac{1}{N_k} \sum_{\mathbf{q}} \delta(E_{\mathbf{k}} - \hbar\Omega - E_{\mathbf{k}-\mathbf{q}}) = \frac{a_l}{2\pi} \int_{-\pi/a_l}^{\pi/a_l} dq \delta\{-2J \cos(ka_l) - \hbar\Omega + 2J \cos[(k-q)a_l]\}. \quad (\text{C2})$$

Next, we exploit the formula

$$\delta[f(x)] = \sum_n \frac{\delta(x - x_n)}{|f'(x_n)|}, \quad (\text{C3})$$

where x_n are zeros of the function $f(x)$. The function $f(q) = -2J \cos(ka_l) - \hbar\Omega + 2J \cos[(k-q)a_l]$ has two zeros $q_{\pm} = k \pm \frac{1}{a_l} \arccos[\cos(ka_l) + \frac{\hbar\Omega}{2J}]$ when $|k| > k_A$, where $k_A = \frac{1}{a_l} \arccos(1 - \frac{\hbar\Omega}{2J})$. Consequently, we obtain

$$\frac{1}{N_k} \sum_{\mathbf{q}} \delta(E_{\mathbf{k}} - \hbar\Omega - E_{\mathbf{k}-\mathbf{q}}) = \frac{1}{2\pi J \sqrt{1 - [\cos(ka_l) + \frac{\hbar\Omega}{2J}]^2}} \quad (\text{C4})$$

when $|k| > k_A$. Otherwise, this sum is equal to zero. In a similar manner, we find

$$\frac{1}{N_k} \sum_{\mathbf{q}} \delta(E_{\mathbf{k}} + \hbar\Omega - E_{\mathbf{k}-\mathbf{q}}) = \frac{1}{2\pi J \sqrt{1 - \left[\cos(ka_l) - \frac{\hbar\Omega}{2J} \right]^2}} \quad (\text{C5})$$

when $|k| < k_B$, where $k_B = \frac{\pi}{a_l} - \frac{1}{a_l} \arccos(1 - \frac{\hbar\Omega}{2J})$. The scattering time is finally given as

$$\tau_k = \begin{cases} \frac{\hbar J}{G^2 n^{\text{ph}}} \sqrt{1 - \left[\cos(ka_l) - \frac{\hbar\Omega}{2J} \right]^2} & \text{if } |k| < k_A, \\ \frac{\hbar J}{G^2} \frac{1}{\frac{n^{\text{ph}}}{\sqrt{1 - \left[\cos(ka_l) - \frac{\hbar\Omega}{2J} \right]^2}} + \frac{n^{\text{ph}+1}}{\sqrt{1 - \left[\cos(ka_l) + \frac{\hbar\Omega}{2J} \right]^2}}} & \text{if } k_A < |k| < k_B, \\ \frac{\hbar J}{G^2 (n^{\text{ph}+1})} \sqrt{1 - \left[\cos(ka_l) + \frac{\hbar\Omega}{2J} \right]^2} & \text{if } |k| > k_B. \end{cases} \quad (\text{C6})$$

The mobility is given as

$$\mu = \frac{\beta}{e_0} \frac{\sum_k n_k \tau_k \mathcal{J}_k^2}{\sum_k n_k}. \quad (\text{C7})$$

For the model at hand, the \mathcal{J}_k term reads $\mathcal{J}_k = \frac{2J e_0 a_l}{\hbar} \sin(ka_l)$. In the limit of low concentration the populations take the form $n_k \propto e^{-\beta E_k}$. After replacing the summation with corresponding integration, we obtain

$$\begin{aligned} \mu = & \frac{e_0 a_l^2}{\hbar} \frac{4\beta J^3}{\pi G^2 I_0 (2\beta J)} \left[\frac{1}{n^{\text{ph}}} \int_0^{k_A a_l} du e^{2\beta J \cos u} \sin^2 u \sqrt{1 - \left(\cos u - \frac{\hbar\Omega}{2J} \right)^2} \right. \\ & + \int_{k_A a_l}^{k_B a_l} du e^{2\beta J \cos u} \sin^2 u \frac{1}{\frac{n^{\text{ph}}}{\sqrt{1 - \left(\cos u - \frac{\hbar\Omega}{2J} \right)^2}} + \frac{n^{\text{ph}+1}}{\sqrt{1 - \left(\cos u + \frac{\hbar\Omega}{2J} \right)^2}}} \\ & \left. + \frac{1}{n^{\text{ph}+1}} \int_{k_B a_l}^{\pi} du e^{2\beta J \cos u} \sin^2 u \sqrt{1 - \left(\cos u + \frac{\hbar\Omega}{2J} \right)^2} \right]. \quad (\text{C8}) \end{aligned}$$

The last formula should be applied only when $\frac{\hbar\Omega}{2J} < 1$. In the opposite case, there exist k points for which electron scattering via phonon emission or absorption is not possible because final-state energy is outside the range of band energies. For these k points, the scattering time calculated using Eq. (C1) is infinite, as well as the mobility obtained using Eq. (C7).

The time given in (C1) is the carrier scattering time. When vertex corrections are included in the formula for the mobility, the momentum relaxation time given as

$$\frac{1}{\tau_{\mathbf{k}}^{(m)}} = \frac{2\pi}{\hbar} \frac{1}{N_k} \sum_{\mathbf{q}} G^2 [(n^{\text{ph}} + 1) \delta(E_{\mathbf{k}} - \hbar\Omega - E_{\mathbf{k}-\mathbf{q}}) (1 - \cos \theta_{\mathbf{k}, \mathbf{k}-\mathbf{q}}) + n^{\text{ph}} \delta(E_{\mathbf{k}} + \hbar\Omega - E_{\mathbf{k}+\mathbf{q}}) (1 - \cos \theta_{\mathbf{k}, \mathbf{k}+\mathbf{q}})], \quad (\text{C9})$$

appears in the expression for mobility Eq. (C7) ($\theta_{\mathbf{k}_1, \mathbf{k}_2}$ is the angle between vectors \mathbf{k}_1 and \mathbf{k}_2 which can take only the values of 0 or π in one dimension). It turns out that these two times are identical for the one-dimensional Holstein model, i.e., $\tau_{\mathbf{k}}^{(m)} = \tau_{\mathbf{k}}$. To show that this is the case, we note that when $|k| > k_A$ the following identity holds:

$$\frac{1}{N_k} \sum_{\mathbf{q}} \delta(E_{\mathbf{k}} - \hbar\Omega - E_{\mathbf{k}-\mathbf{q}}) (1 - \cos \theta_{k, k-q}) = \frac{\int_{-\pi/a_l}^{\pi/a_l} dq [\delta(q - q_+) (1 - \cos \theta_{k, k-q_+}) + \delta(q - q_-) (1 - \cos \theta_{k, k-q_-})]}{4\pi J \sqrt{1 - \left[\cos(ka_l) + \frac{\hbar\Omega}{2J} \right]^2}}. \quad (\text{C10})$$

Since one of the $\cos \theta_{k, k-q_{\pm}}$ terms is equal to 1 and the other is equal to -1 , the last expression reduces to

$$\frac{1}{N_k} \sum_{\mathbf{q}} \delta(E_{\mathbf{k}} - \hbar\Omega - E_{\mathbf{k}-\mathbf{q}}) (1 - \cos \theta_{k, k-q}) = \frac{1}{2\pi J \sqrt{1 - \left[\cos(ka_l) + \frac{\hbar\Omega}{2J} \right]^2}}, \quad (\text{C11})$$

which is the same as (C4). In a similar manner one can show that other relevant terms in the evaluation of $\tau_{\mathbf{k}}^{(m)}$ and $\tau_{\mathbf{k}}$ are the same.

APPENDIX D: CALCULATION OF MOBILITY FOR NARROW LINEWIDTHS OF THE SPECTRAL FUNCTION

To evaluate the mobility in this case we start from Eqs. (39)–(43). We also make use of the fact that in the case of a single-phonon mode, the function $\theta_{\mathbf{X},\mathbf{Y},\mathbf{Z}}(t)\theta_{\mathbf{X}}^{(0)}\theta_{\mathbf{Y}}^{(0)}$ is periodic in time with period $\frac{2\pi}{\Omega}$ and we represent it using the Fourier series

$$\theta_{\mathbf{X},\mathbf{Y},\mathbf{Z}}(t)\theta_{\mathbf{X}}^{(0)}\theta_{\mathbf{Y}}^{(0)} = \sum_n c_{\mathbf{X},\mathbf{Y},\mathbf{Z}}^{(n)} e^{in\Omega t} \quad (\text{D1})$$

with

$$c_{\mathbf{X},\mathbf{Y},\mathbf{Z}}^{(n)} = \frac{\Omega}{2\pi} \int_{-\pi/\Omega}^{\pi/\Omega} dt e^{-in\Omega t} \theta_{\mathbf{X},\mathbf{Y},\mathbf{Z}}(t)\theta_{\mathbf{X}}^{(0)}\theta_{\mathbf{Y}}^{(0)}. \quad (\text{D2})$$

The mobility then reads

$$\begin{aligned} \mu_{ii} &= \frac{\beta e_0}{4\pi N_c \hbar^2} \sum_{\mathbf{k}_1, \mathbf{k}_2} \sum_n f_{ii}(\mathbf{k}_1, \mathbf{k}_2, n) \\ &\times \int d\omega n_F(\omega) A_{\mathbf{k}_1}(\omega) A_{\mathbf{k}_2}(\omega + n\Omega), \end{aligned} \quad (\text{D3})$$

where

$$\begin{aligned} f_{ii}(\mathbf{k}_1, \mathbf{k}_2, n) &= -\frac{1}{N_k} \sum_{\mathbf{X}, \mathbf{Y}, \mathbf{Z}} J_{\mathbf{X}} J_{\mathbf{Y}}(\mathbf{X})_i(\mathbf{Y})_i e^{ik_1(\mathbf{Y}+\mathbf{Z})} e^{ik_2(\mathbf{X}-\mathbf{Z})} c_{\mathbf{X},\mathbf{Y},\mathbf{Z}}^{(n)}. \end{aligned} \quad (\text{D4})$$

We find that the most significant contribution to the mobility comes from the term with $\mathbf{k}_1 = \mathbf{k}_2$ and $n = 0$ in Eq. (D3). Making use of the spectral function given in Eq. (70) we find in this case

$$\begin{aligned} &\int d\omega n_F(\omega) A_{\mathbf{k}_1}(\omega) A_{\mathbf{k}_2}(\omega + n\Omega) \\ &= \int d\omega n_F(\omega) A_{\mathbf{k}_1}(\omega)^2 \\ &= \pi^2 \alpha_{\mathbf{k}}^2 e^{-\beta e_{\mathbf{k}}} \frac{4\alpha_{\mathbf{k}}}{4\alpha_{\mathbf{k}}^2 - \beta^2} \end{aligned} \quad (\text{D5})$$

and

$$N_c = \frac{1}{2\pi} \int d\omega n_F(\omega) A_{\mathbf{k}}(\omega) = \sum_{\mathbf{k}} e^{-\beta e_{\mathbf{k}}} \frac{\alpha_{\mathbf{k}}^2}{\alpha_{\mathbf{k}}^2 - \beta^2}. \quad (\text{D6})$$

The mobility then reads

$$\mu_{ii} = \frac{\beta e_0}{4\pi \hbar^2} \frac{\sum_{\mathbf{k}} f(\mathbf{k}, \mathbf{k}, 0) \pi^2 e^{-\beta e_{\mathbf{k}}} \frac{4\alpha_{\mathbf{k}}^3}{4\alpha_{\mathbf{k}}^2 - \beta^2}}{\sum_{\mathbf{k}} e^{-\beta e_{\mathbf{k}}} \frac{\alpha_{\mathbf{k}}^2}{\alpha_{\mathbf{k}}^2 - \beta^2}}. \quad (\text{D7})$$

APPENDIX E: EVALUATION OF THE $\Sigma^{(a)}$ SUMS

In this section, we present the numerical procedure that we used to evaluate the sums given in Eq. (69) that we repeat here:

$$\Sigma_{\mathbf{k}}^{(a)} = \frac{1}{N_k} \sum_{\mathbf{q}} \frac{\chi^{(a)}(\mathbf{k}, \mathbf{q})}{\frac{e_{\mathbf{k}} - e_{\mathbf{k}+\mathbf{q}}}{\hbar} + n\Omega - i\text{Im}\Sigma_{\mathbf{k}+\mathbf{q}}}. \quad (\text{E1})$$

We first transform the sum into an integral and obtain in the one-dimensional case

$$\Sigma_k^{(a)} = \frac{a_l}{2\pi} \int_{-\pi/a_l}^{\pi/a_l} dq \frac{\chi^{(a)}(k, q)}{\frac{e_k - e_{k+q}}{\hbar} + n\Omega - i\text{Im}\Sigma_{k+q}}. \quad (\text{E2})$$

The interval $(-\pi/a_l, \pi/a_l)$ was then divided into N_k equal intervals and the integral was rewritten as

$$\Sigma_k^{(a)} = \frac{a_l}{2\pi} \sum_{i=0}^{N-1} \int_{q_i}^{q_{i+1}} dq \frac{\chi^{(a)}(k, q)}{\frac{e_k - e_{k+q}}{\hbar} + n\Omega - i\text{Im}\Sigma_{k+q}}, \quad (\text{E3})$$

where $q_i = -\pi/a_l + \frac{i}{N}\pi/a_l$. To evaluate the integral

$$I_i = \int_{q_i}^{q_{i+1}} dq \frac{\chi^{(a)}(k, q)}{\frac{e_k - e_{k+q}}{\hbar} + n\Omega - i\text{Im}\Sigma_{k+q}}, \quad (\text{E4})$$

we note that the functions $\chi^{(a)}(k, q)$, e_{k+q} , and Σ_{k+q} are slowly varying functions of q . However, since the denominator can take the values close to zero, the whole function under the integral can vary rapidly with q . We introduce the quantities

$$\bar{\chi} = \frac{1}{2} [\chi(k, q_i) + \chi(k, q_{i+1})], \quad (\text{E5})$$

$$\bar{\Sigma} = \frac{1}{2} [\Sigma(k + q_i) + \Sigma(k + q_{i+1})], \quad (\text{E6})$$

and we perform linear interpolation of e_{k+q} as

$$e_{k+q} = e_{k+q_i} + (q - q_i) \frac{e_{k+q_{i+1}} - e_{k+q_i}}{q_{i+1} - q_i}. \quad (\text{E7})$$

We then approximate the integral as

$$\begin{aligned} I_i &\approx \bar{\chi} \int_{q_i}^{q_{i+1}} dq \\ &\times \frac{1}{\frac{e_k}{\hbar} + n\Omega - \left[\frac{e_{k+q_i}}{\hbar} + \frac{1}{\hbar}(q - q_i) \frac{e_{k+q_{i+1}} - e_{k+q_i}}{q_{i+1} - q_i} \right] - i\text{Im}\bar{\Sigma}}. \end{aligned} \quad (\text{E8})$$

The integral is then of the form

$$I_i = \bar{\chi} \int_{q_i}^{q_{i+1}} dq \frac{1}{A + B(q - q_i) + iC} \quad (\text{E9})$$

with $A = \frac{e_k}{\hbar} + n\Omega - \frac{e_{k+q_i}}{\hbar}$, $B = -\frac{1}{\hbar} \frac{e_{k+q_{i+1}} - e_{k+q_i}}{q_{i+1} - q_i}$, $C = -i\text{Im}\bar{\Sigma}$. Evaluation of the integral leads to the result

$$\begin{aligned} I_i &= \frac{\bar{\chi}}{B} \left[\frac{1}{2} \ln(v^2 + C^2) \right]_{v=A}^{v=A+B(q_{i+1}-q_i)} \\ &- i \arctan \frac{v}{C} \Big|_{v=A}^{v=A+B(q_{i+1}-q_i)}. \end{aligned} \quad (\text{E10})$$

- [1] N. W. Ashcroft and N. D. Mermin, *Solid State Physics* (Harcourt, Orlando, 1976).
- [2] S. Baroni, S. de Gironcoli, A. Dal Corso, and P. Giannozzi, *Rev. Mod. Phys.* **73**, 515 (2001).
- [3] F. Giustino, *Rev. Mod. Phys.* **89**, 015003 (2017).
- [4] F. Giustino, M. L. Cohen, and S. G. Louie, *Phys. Rev. B* **76**, 165108 (2007).
- [5] J. Noffsinger, F. Giustino, B. D. Malone, C.-H. Park, S. G. Louie, and M. L. Cohen, *Comput. Phys. Commun.* **181**, 2140 (2010).
- [6] C. Verdi and F. Giustino, *Phys. Rev. Lett.* **115**, 176401 (2015).
- [7] J. Sjakste, N. Vast, M. Calandra, and F. Mauri, *Phys. Rev. B* **92**, 054307 (2015).
- [8] B. Liao, J. Zhou, B. Qiu, M. S. Dresselhaus, and G. Chen, *Phys. Rev. B* **91**, 235419 (2015).
- [9] T. Gunst, T. Markussen, K. Stokbro, and M. Brandbyge, *Phys. Rev. B* **93**, 035414 (2016).
- [10] J.-J. Zhou and M. Bernardi, *Phys. Rev. B* **94**, 201201 (2016).
- [11] C.-H. Park, N. Bonini, T. Sohler, G. Samsonidze, B. Kozinsky, M. Calandra, F. Mauri, and N. Marzari, *Nano Lett.* **14**, 1113 (2014).
- [12] N. Sule and I. Knezevic, *J. Appl. Phys.* **112**, 053702 (2012).
- [13] T. Holstein, *Ann. Phys.* **8**, 343 (1959).
- [14] I. G. Lang and Y. A. Firsov, *Sov. Phys. JETP* **16**, 1301 (1963).
- [15] G. Wellein, H. Röder, and H. Fehske, *Phys. Rev. B* **53**, 9666 (1996).
- [16] G. Wellein and H. Fehske, *Phys. Rev. B* **56**, 4513 (1997).
- [17] M. Capone, W. Stephan, and M. Grilli, *Phys. Rev. B* **56**, 4484 (1997).
- [18] E. Jeckelmann and S. R. White, *Phys. Rev. B* **57**, 6376 (1998).
- [19] C. Zhang, E. Jeckelmann, and S. R. White, *Phys. Rev. Lett.* **80**, 2661 (1998).
- [20] R. J. Bursill, R. H. McKenzie, and C. J. Hamer, *Phys. Rev. Lett.* **80**, 5607 (1998).
- [21] A. H. Romero, D. W. Brown, and K. Lindenberg, *J. Chem. Phys.* **109**, 6540 (1998).
- [22] G. Wellein and H. Fehske, *Phys. Rev. B* **58**, 6208 (1998).
- [23] J. Bonča, S. A. Trugman, and I. Batistić, *Phys. Rev. B* **60**, 1633 (1999).
- [24] L.-C. Ku, S. A. Trugman, and J. Bonča, *Phys. Rev. B* **65**, 174306 (2002).
- [25] M. Hohenadler, H. G. Evertz, and W. von der Linden, *Phys. Rev. B* **69**, 024301 (2004).
- [26] S. Ciuchi, F. de Pasquale, S. Fratini, and D. Feinberg, *Phys. Rev. B* **56**, 4494 (1997).
- [27] S. Fratini and S. Ciuchi, *Phys. Rev. Lett.* **91**, 256403 (2003).
- [28] J. E. Hirsch, R. L. Sugar, D. J. Scalapino, and R. Blankenbecler, *Phys. Rev. B* **26**, 5033 (1982).
- [29] H. De Raedt and A. Lagendijk, *Phys. Rev. B* **27**, 6097 (1983).
- [30] R. H. McKenzie, C. J. Hamer, and D. W. Murray, *Phys. Rev. B* **53**, 9676 (1996).
- [31] P. E. Spencer, J. H. Samson, P. E. Kornilovitch, and A. S. Alexandrov, *Phys. Rev. B* **71**, 184310 (2005).
- [32] A. S. Mishchenko, N. Nagaosa, G. De Filippis, A. de Candia, and V. Cataudella, *Phys. Rev. Lett.* **114**, 146401 (2015).
- [33] G. L. Goodvin, A. S. Mishchenko, and M. Berciu, *Phys. Rev. Lett.* **107**, 076403 (2011).
- [34] G. De Filippis, V. Cataudella, A. S. Mishchenko, and N. Nagaosa, *Phys. Rev. B* **85**, 094302 (2012).
- [35] M. Grover and R. Silbey, *J. Chem. Phys.* **54**, 4843 (1971).
- [36] D. R. Yarkony and R. Silbey, *J. Chem. Phys.* **67**, 5818 (1977).
- [37] R. Silbey and R. W. Munn, *J. Chem. Phys.* **72**, 2763 (1980).
- [38] Y.-C. Cheng and R. J. Silbey, *J. Chem. Phys.* **128**, 114713 (2008).
- [39] K. Hannewald and P. A. Bobbert, *Phys. Rev. B* **69**, 075212 (2004).
- [40] F. Ortman, F. Bechstedt, and K. Hannewald, *Phys. Rev. B* **79**, 235206 (2009).
- [41] R. P. Feynman, R. W. Hellwarth, C. K. Iddings, and P. M. Platzman, *Phys. Rev.* **127**, 1004 (1962).
- [42] A. Ishihara, *J. Phys. A: Gen. Phys.* **1**, 539 (1968).
- [43] G. Mahan, *Many-Particle Physics* (Kluwer Academic, New York, 2000).
- [44] Q. Liu, *Phys. Lett. A* **376**, 1219 (2012).
- [45] V. M. Stojanović, P. A. Bobbert, and M. A. J. Michels, *Phys. Rev. B* **69**, 144302 (2004).
- [46] M. Capone, S. Ciuchi, and C. Grimaldi, *Europhys. Lett.* **42**, 523 (1998).
- [47] B. Gerlach and H. Löwen, *Phys. Rev. B* **35**, 4291 (1987).
- [48] A. Troisi and G. Orlandi, *Phys. Rev. Lett.* **96**, 086601 (2006).
- [49] H. Ishii, K. Honma, N. Kobayashi, and K. Hirose, *Phys. Rev. B* **85**, 245206 (2012).
- [50] L. Wang, O. V. Prezhdo, and D. Beljonne, *Phys. Chem. Chem. Phys.* **17**, 12395 (2015).
- [51] L. Wang and D. Beljonne, *J. Phys. Chem. Lett.* **4**, 1888 (2013).
- [52] L. A. Ribeiro and S. Stafström, *Phys. Chem. Chem. Phys.* **18**, 1386 (2016).
- [53] P. V. Parandekar and J. C. Tully, *J. Chem. Phys.* **122**, 094102 (2005).
- [54] J. C. Tully, *J. Chem. Phys.* **93**, 1061 (1990).
- [55] L. Song and Q. Shi, *J. Chem. Phys.* **142**, 174103 (2015).
- [56] G. Nan, X. Yang, L. Wang, Z. Shuai, and Y. Zhao, *Phys. Rev. B* **79**, 115203 (2009).
- [57] S. H. Lin, C. H. Chang, K. K. Liang, R. Chang, Y. J. Shiu, J. M. Zhang, T.-S. Yang, M. Hayashi, and F. C. Hsu, Ultrafast dynamics and spectroscopy of bacterial photosynthetic reaction centers, in *Advances in Chemical Physics* (John Wiley & Sons, Inc., 2002), pp. 1–88.
- [58] X. Yang, L. Wang, C. Wang, W. Long, and Z. Shuai, *Chem. Mater.* **20**, 3205 (2008).
- [59] A. N. Sokolov, S. Atahan-Evrenk, R. Mondal, H. B. Akkerman, R. S. Sánchez-Carrera, S. Granados-Focil, J. Schrier, S. C. B. Mannsfeld, A. P. Zoombelt, Z. Bao, and A. Aspuru-Guzik, *Nat. Commun.* **2**, 437 (2011).
- [60] S.-H. Wen, A. Li, J. Song, W.-Q. Deng, K.-L. Han, and W. A. Goddard, *J. Phys. Chem. B* **113**, 8813 (2009).
- [61] V. Coropceanu, J. Cornil, D. A. da Silva Filho, Y. Olivier, R. Silbey, and J.-L. Bredas, *Chem. Rev.* **107**, 926 (2007).
- [62] B. Baumeier, J. Kirkpatrick, and D. Andrienko, *Phys. Chem. Chem. Phys.* **12**, 11103 (2010).
- [63] N. Prodanović, N. Vukmirović, Z. Ikonić, P. Harrison, and D. Indjin, *J. Phys. Chem. Lett.* **5**, 1335 (2014).
- [64] M. Kornjača and N. Vukmirović, *Ann. Phys.* **391**, 183 (2018).
- [65] R. W. Munn and R. Silbey, *J. Chem. Phys.* **83**, 1843 (1985).
- [66] R. W. Munn and R. Silbey, *J. Chem. Phys.* **83**, 1854 (1985).
- [67] D. Chen, J. Ye, H. Zhang, and Y. Zhao, *J. Phys. Chem. B* **115**, 5312 (2011).
- [68] G. De Filippis, V. Cataudella, A. S. Mishchenko, N. Nagaosa, A. Fierro, and A. de Candia, *Phys. Rev. Lett.* **114**, 086601 (2015).